Supporting Information

Metabolic sensor governing bacterial virulence in *Staphylococcus aureus*

Yue Ding[a], Xing Liu[b], Feifei Chen[a], Hongxia Di[a], Bin Xu[a], Lu Zhou[c], Xin Deng[d,e], Min Wu[f], Cai-Guang Yang [b,1], Lefu Lan[a,1]

[a]Department of Molecular Pharmacology, Shanghai Institute of Materia Medica, Chinese Academy of Sciences, Shanghai 201203, China;

[b]CAS Key Laboratory of Receptor Research, Shanghai Institute of Materia Medica, Chinese Academy of Sciences, Shanghai 201203, China;

[c]Department of Medicinal Chemistry, School of Pharmacy, Fudan University, Shanghai 201203, China;

[d]Department of Chemistry and [e]Institute for Biophysical Dynamics, The University of Chicago, Chicago, Illinois 60637, USA;

[f]Department of Basic Sciences, University of North Dakota School of Medicine and Health Sciences, Grand Forks, ND 58203, USA.

The authors declare no conflict of interest.

[1]To whom correspondence should be addressed:

Shanghai Institute of Materia Medica, Chinese Academy of Sciences, Shanghai 201203, China. Phone: 021-50803109; Fax: 021-50807088; Email: yangcg@simm.ac.cn (C.-G.Y.) or llan@mail.shcnc.ac.cn (L.L.)

Running Title: CcpE links TCA-cycle activity with virulence

Experimental Procedures

Construction of *S. aureus* Δ*ccpE* Strain, Δ*citB* Strain, and Δ*ccpE*Δ*citB* Double Mutant Strain. The gene replacement vector pKOR1 (1) was used to construct a *ccpE* (*NWMN_0641*) null mutant strain (Δ*ccpE*) as described in our previous studies (2, 3). Briefly, PCRs were performed in order to amplify sequences upstream (ca. 1.55 kb) and downstream (ca. 2.0 kb) of the intended deletion. The upstream fragment was amplified from *S. aureus* strain Newman genomic DNA using primers ccpE-up-F (with *Bam*HI site) and ccpE-up-R (with *Hin*dIII site) (Table S2), and the downstream fragment was amplified with primers ccpE-down-F (with *Hin*dIII site) and ccpE-down-R (with *Xho*I site) (Table S2). A ca.1.3 kb erythromycin resistance cassette (covering 465 bp of the *ermB* upstream region, the 738bp *ermB* gene, and 60 bp downstream of *ermB* gene) was amplified from plasmid pAT18 (4) with primers erm-F and erm-R (both with *Hin*dIII site) (Table S2) for replacing the *ccpE* gene in the *S. aureus* Newman strain. The three PCR products were digested with *Hin*dIII, mixed together and ligated by T4 DNA ligase (New England Biolabs). The ligation product was amplified with primers ccpE-BP-F and ccpE-BP-R (Table S2). Next, the PCR product was used for recombination with pKOR1, and the product was introduced to *E. coli* DH5α. The construct was sequenced to ensure that no unwanted mutations resulted. The resulting plasmid, pKOR1::Δ*ccpE*, was transferred by electroporation to *S. aureus* RN4220, and subsequently into *S. aureus* Newman. The allelic replacement was performed as described previously and PCR and DNA sequencing further confirmed the deletion of *ccpE*.

To construct a *citB* (*NWMN_1263*) null mutant strain, PCRs were performed in order to amplify sequences upstream (ca. 1.95 kb) and downstream (ca. 2.0 kb) of the intended deletion. The upstream fragment was amplified from *S. aureus* strain Newman genomic DNA using primers citB-up-F (with *Nde*I site) and citB-up-R (with *Bam*HI site) (Table S2), and the upstream fragment was amplified with primers citB-down-F (with *Bam*HI site) and citB-down-R (with *Xho*I site) (Table S2). The two fragments were digested with *Bam*HI and ligated. The ligation product was then PCR amplified with primers citB-BP-F and citB-BP-F (Table S2), and subsequently recombined into pKOR1 to generate pKOR1::Δ*citB*. The Δ*citB* mutant was constructed according to a similar strategy as described above.

The Δ*ccpE*Δ*citB* double mutant strain (Table S1) was generated by Ø85 phage transduction (2, 5) of the Δ*ccpE*::*ermB* allele from Newman Δ*ccpE* strain (Table S1) into the Δ*citB* background (Table S1). Strain inactivated for *ccpE* in JE2 was generated by transduction of the Δ*ccpE*::*ermB* allele from Newman Δ*ccpE* using bacteriophage Ø85. All mutant alleles were verified by DNA sequencing.

Construction of Plasmids for Constitutive Expression of *ccpE*, $ccpE_{R145A}$, $ccpE_{R256A}$, and *citB*. To construct plasmids for constitutive expression of *ccpE*, $ccpE_{R145A}$, $ccpE_{R256A}$, and *citB*, shuttle plasmid pYJ335 (6) was used as described in our previous studies (2, 3, 5). To express *ccpE* constitutively, a ca. 0.9 kb DNA fragment containing *ccpE* was amplified from *S. aureus* Newman genomic DNA with primers ccpE-F and ccpE-R (Table S2) and then cloned into pYJ335, where the *ccpE*

gene was downstream of the tetracycline-inducible *xyl*/*tetO* promoter, yielding plasmid p-*ccpE* (Table S1). In order to express *ccpE* in the Δ*ccpE* strain (with an erythromycin resistance marker) that harbors the derivates of pCL-lacZ (with a chloroamphenicol resistance marker), plasmid pT-*ccpE* was constructed. Briefly, ca. 0.9 kb DNA fragment containing *ccpE* was amplified from *S. aureus* Newman genomic DNA with primers ccpE-F and ccpE-R-tet (with *Eco*RI site) (Table S2), and a 1.6 kb tetracycline resistance cassette was amplified from plasmid pT181 (7) with primers tet-F (with *Eco*RI site) and tet-R (Table S2). These two PCR products were digested with *Eco*RI, mixed together, and ligated by T4 DNA ligase. The ligation product was amplified with primers ccpE-F and tet-R and then cloned into pYJ335, where the *ccpE* gene was downstream of the tetracycline-inducible *xyl*/*tetO* promoter, yielding plasmid pT-*ccpE* (Table S1). Plasmid pYJ335-Tc (Table S1) was constructed by cloning the tetracycline resistance cassette (amplified from plasmid pT181 with primers tet-F and tet-R) into pYJ335 and this plasmid was used as the control plasmid where appropriate.

Two mutations, pT-$CcpE_{R145A}$ and pT-$CcpE_{R256A}$ (Table S1), were constructed using a QuikChange II site-directed mutagenesis kit (Stratagene) with primer pairs R145AF/R145AR and R256AF/R256AR, respectively. To express *citB*, a ca. 2,8 kb DNA fragment (covering 108 bp upstream and 52 bp downstream of *citB* gene) was generated from *S. aureus* Newman genomic DNA with primers citB-F and citB-R (Table S2) and then cloned into pYJ335 in the same orientation as the tetracycline-inducible *xyl*/*tetO* promoter, yielding plasmid p-*citB* (Table S1). All of the

constructs were sequenced to ensure that no unwanted mutations were introduced.

Construction of *citB-lacZ*, *citB-M-lacZ*, *cap-lacZ*, *SAV1168-lacZ*, *SAV1168-M-lacZ*, and *crtO-lacZ* transcriptional fusions. The plasmid pCL-LacZ carrying a promoterless *lacZ* reporter gene cluster was used to construct promoter-*lacZ* reporter fusions as described previously (8). For *citB-lacZ*, the *citB* promoter region (-767 to +78 of the start codon) was amplified by PCR using the primers lacZ1350-F (with *Eco*RI site) and lacZ1350-R (with *Kpn*I site) (Table S2). To generate *citB-M-lacZ* (ATAAGTTTTGCTTAT was mutated to ***CGCCAC***TTTGCTTAT), a QuikChange II site-directed mutagenesis kit (Stratagene) and primer pair citB-M-F/citB-M-R (Table S2) were used. For *cap-lacZ*, the *cap* promoter region (-406 to +178 of the start codon) was amplified by PCR using the primers lacZ0149-F (with *Eco*RI site) and lacZ0149-R (with *Kpn*I site) (Table S2). For *SAV1168-lacZ*, the *SAV1168* promoter region (-511 to +158 of the start codon) was amplified by PCR using the primers lacZ1168-F (with *Eco*RI site) and lacZ1168-R (with *Kpn*I site) (Table S2). To generate *SAV1168-M-lacZ* (ATGATAAGTTTTGCTTAAATA was mutated to ATGATAAGTTTTATGGCCATA), a QuikChange II site-directed mutagenesis kit (Stratagene) and primer pair 1168M1F /1168M1R (Table S2) were used. For *crtO-lacZ*, the *crtO* promoter region (-766 to +10 of the start codon) was amplified by PCR using the primers lacZ-crtO-F (with *Eco*RI site) and lacZ-crtO-R (with *Kpn*I site) (Table S2). All promoter DNA fragments were amplified from *S. aureus* Newman genomic DNA. The cloned promoter

sequences were confirmed by DNA sequencing. The constructs were electroporated into RN4220 and then transformed into Newman and its derivates using bacteriophage Ø85, as indicated.

β-Galactosidase assays. Briefly, overnight cultures of the indicated strains were washed twice and diluted 100-fold in fresh TSB medium. The liquid cultures were grown in a 20-ml tube with a tube volume-to-medium volume ratio of 5:1, shaking with 250 rpm at 37 ℃, and sampled at time points thereafter. β-Galactosidase activity was assayed as previously described (9) using 4-methylumbelliferyl-β-d-galactoside (4MUG) as the enzymatic substrate. The product (7-hydroxy-4-methylcoumarin, 4MU) was detected using a 2104 EnVision® Multilabel Plate Readers or Synergy 2 (Biotek) following the manufacturer's instructions. The reaction was monitored at 460 nm with an excitation wavelength of 365 nm. Each sample was tested in triplicate. Relative LacZ activity was normalized by cell density at 600 nm.

Protein Expression and Purification. The *ccpE* gene was amplified using genomic DNA from *S. aureus* Newman as a template with primers ccpE-PF (with *Bam*HI site) and ccpE-PR (with *Xho*I site) (Table S2). The amplified fragment was digested with *Bam*HI and *Xho*I and inserted into pET28a digested with the same pair of restriction enzymes in order to generate pET28a::*ccpE* (Table S1). Two mutations, pET28a::$CcpE_{R145A}$ and pET28a::$CcpE_{R256A}$ (Table S1), were constructed using a QuikChange II site-directed mutagenesis kit (Stratagene) with primer pairs

R145AF/R145AR and R256AF/R256AR (Table S2), respectively.

The proteins were expressed in *E. coli* strain BL21 star (DE3) and purifications were performed as described in our previous studies (2, 3, 9). Briefly, the *E. coli* strain was sub-cultured into 200 ml of LB broth (with appropriate antibiotics) to obtain an optical density at 600 nm (OD600) of approximately 0.1 and grown to an OD600 of ~0.6. Expression of CcpE was induced with 1 mM isopropyl-β-D-thiogalactoside (IPTG) overnight at 16 ℃ with shaking (250 rpm). Cells were harvested, and the pellets were suspended in 4 ml of buffer A (20 mM Tris-HCl, pH 8.0, 500 mM NaCl, 20 mM EDTA, 1 mM DTT), and lysed at 4 ℃ by sonication. The lysate was centrifuged at 15,000 *g* for 30 min, and the supernatants were loaded onto a nickel-nitrilotriacetic acid column (His Trap; GE Healthcare). After being equilibrated with buffer A, 6His-CcpE was eluted with a 0-100% gradient of buffer B (20 mM Tris-HCl, pH 8.0; 500 mM NaCl, 1 mM DTT, 500 mM Imidazole). The purified protein was verified by SDS-PAGE followed by Coomassie blue staining. A similar strategy was used for protein expression and purification of 6His-$CcpE_{R145A}$ and 6His-$CcpE_{R256A}$.

The proteins were finally purified and their oligomerization states were estimated by size-exclusion chromatography using a calibrated HiLoad 16/600 Superdex 200 pg (GE Healthcare, 28-9893-35) pre-equilibrated with buffer C (20 mM Tris-HCl, pH 8.0, 500 mM NaCl, and 1 mM DTT). The column was calibrated using gel-filtration calibration kits (28-4038-42) from GE Healthcare and the results were analyzed according to the manual using Microsoft Excel. Sample fractions were analyzed for

purity by SDS-PAGE and pure fractions were pooled and concentrated. Blue Dextran 2000 was used to calculate the void volume of the column.

Fluorescence-based Thermal Shift (FTS) assay. FTS assays were performed as described in our previous study (10) with some modifications. Purified 6His-CcpE was appropriately diluted in a buffer containing 20 mM Tris-HCl, pH 8.0, 500 mM NaCl, and 1 mM DTT. All assay experiments used 4 μg proteins per well and 5 nl 5000× Sypro Orange (Invitrogen) up to a total volume of 20 μl. 96-well PCR plates were sealed with optical seal, shaken, and centrifuged after the protein and the compounds were added. Thermal scanning (25 to 95℃ at 1℃/min) was performed using a Fast 7500 Real-Time PCR System (Applied Biosystems) and fluorescence intensity was measured after every 20 seconds. Curve fitting, melting temperature calculation, and report generation on the raw FTS data were performed using Protein thermal shift software (Applied Biosystems). All experiments were performed in triplicate. Data analysis was analyzed with Origin software. Pre-melt (initial) and post-melt (final) fluorescence signals of all samples have been normalized to relative values of 0% and 100%, respectively.

Electrophoretic Mobility Shift Assay (EMSA). The electrophoretic mobility shift assays (EMSA) were performed as described in our previous studies (2, 3, 9) with some modifications. Briefly, a mixture of the DNA probe, control DNA fragments, purified proteins, and binding buffer A (20mM Tris-HCl, pH 7.4; 50 mM KCl, 20 mM

$MgCl_2$, 1 mM EDTA, 5% Nonidet® P-40, and 5% Glycerol) were incubated on ice for 30 min. Reaction mixtures were loaded onto a 4.5% nondenaturing polyacrylamide gel in 0.5×TBS buffer (50 mM Tris, 41.5 mM borate, pH 8.0). The gels were run at 300V for 5 min and at 80V at 4℃ for the remaining time. The gel was stained in GelRed nucleic acid staining solution (Biotium, 41003) for 10 min, and then the DNA bands were visualized by gel exposure to 260-nm UV light using Tanon-5200 multi. To evaluate the effect of sodium citrate (Sigma-Aldrich, W302600) and sodium isocitrate (Sigma-Aldrich, I1252) on the protein-DNA interaction, either sodium citrate or sodium isocitrate was added to the binding reaction buffer at a final concentration of 10 mM. The electrophoretic mobility shift experiments were also performed in a similar strategy with a binding buffer B consisting of 10mM Tris-HCl (pH 7.5), 50 mM NaCl, 1mM EDTA, 1mM DTT, and 5% Glycerol. This binding buffer is similar to the buffer that was used in a recent study for EMSA to evaluate the CcpE-protein interactions. Images were taken using Tanon-5200 multi.

DNA probes were PCR-amplified from *S. aureus* Newman genomic DNA using the primers listed in Table S6. The probes for the *citB* (*SAV1350*) promoter, a 282 bp DNA fragment (*citB-L-p*) covering the promoter regions of *citB* (from -194 to +88 of the start codon which contains protected region I but not protected region II) was amplified with primers citB-p-F and citB-p-R (Table S2). The *citB* promoter DNA *citB-p12* fragment (from -321 to +66 of the start codon, covering both protected regions I and II) was amplified with primers citB-12F and citB-12F (Table S2). For *cap5A* (*SAV0149*) promoter, a ca. 0.37 kb DNA fragment (*cap5A-p*) covering the

promoter regions of *cap5A* (from −211 to +163 of the start codon) was amplified using primers cap-p-F and cap-p-R (Table S2). For *SAV1168* promoter, a ca. 0.38 kb DNA fragment (*SAV1168-p*) covering the promoter regions of *SAV1168* (from −150 to +158 of the start codon) was amplified using primers SAV1168-p-F and SAV1168-p-R. The PCR products were purified with DNA products purification kit (Omega, D6492-02).

To test the role of the Box I-like sequences (ATAA-N_7-TTAT, where N is any nucleotide) in the interaction between *citB* promoter DNA and CcpE, a ca. 0.24 kb DNA fragment (*citB-p*) covering the promoter region of *citB* (from -151 to +88 of the start codon) was amplified from *S. aureus* Newman genomic DNA with primers citB-pB-F and citB-p-R (Table S2) while a ca. 0.24 kb mutated DNA fragment (*citB-M-p*, ATAAGTTTTGCTTAT was mutated to *CGCCAC*TTTGCTTAT) was amplified with primers citB-pM-F and citB-p-R (Table S2).

Additionally, DNA fragments, including *ccpE-O* (from +94 to +532 of the start codon of *ccpE*) and *citB-U* (from -128 to +88 of the start codon of *citB*), were used as a negative control where appropriate. For *ccpE-O*, primers ccpE-cF and ccpE-cR (Table S2) were used. For *citB-U*, primers citB-pc-F and citB-p-R (Table S2) were used.

Dye Primer-based DNase I Footprinting Assay. The published DNase I footprint protocol (11) was modified in a similar way as described in our previous study (3, 9, 12). Briefly, PCR was used to generate DNA fragments using the primer sets as

detailed in Table S2. For amplification of *citB* promoter, a ca. 0.85 kb DNA fragment (from −766 to +88 of the start codon of *citB*) was generated by PCR using primers 1350FAM and lacZ1350-F. For amplification of the *SAV1168* promoter, a ca. 0.67 kb DNA fragment (from −511 to +158 of the start codon of *SAV1168*) was generated by PCR with primer 1168FAM and lacZ1168-F. All PCR products were purified with a DNA products purification kit (Omega, D6492-02). 50 nM 6-carboxyfluorescein (6-FAM)-labeled promoter DNA and 2 μM 6His-CcpE in 50 μl of binding buffer (20 mM Tris-HCl, pH 7.4; 50 mM KCl, 20 mM $MgCl_2$, 1 mM EDTA, and 5% Nonidet® P-40, 1 mM DTT) were incubated on ice for 30 min. Then 0.01 unit of DNase I was added to the reaction mixture and incubated for 5 more min. The digestion was terminated by adding 90 μl of quenching solution (200 mM NaCl, 30 mM EDTA, 1% SDS), and then the mixture was extracted with 200 μl of phenol-chloroform-isoamyl alcohol (25:24:1). The digested DNA fragments were isolated by ethanol precipitation. 5.0 μl of digested DNA was mixed with 4.9 μl of HiDi formamide and 0.1 μl of GeneScan-500 LIZ size standards (Applied Biosystems). A 3730XL DNA analyzer detected the sample, and the result was analyzed with GeneMapper software. The dye primer-based sequencing kit (Thermo, 79260) was used in order to more precisely determine the sequences after the capillary electrophoresis results of the reactions were aligned. Electrophoregrams were then analyzed with GeneMarker v1.8 (Applied Biosystems).

Measurement of Intracellular Citrate Concentration. Overnight cultures of the

indicated *S. aureu* strains were washed twice and diluted 100-fold in fresh TSB medium without glucose. The liquid cultures were grown in a 50-ml tube with a volume-to-medium volume ratio of 5:1, shaken at 250 rpm at 37℃ for 6 h (OD600 ≈ 5.0), of aeration. After collection of the cells by centrifugation, the pellet was washed with 20 mM Tris-HCl (pH 8.0) containing 1 mM EDTA, and resuspended in 0.01 M PBS buffer (137 mM NaCl, 2.7 mM KCl, 4.3 mM Na_2HPO_4, 1.4 mM KH_2PO_4; pH=7.4). This mixture was subjected to homogenizer lysis (FastPrep FP2400, QBiogene, USA; 3 cycles each of 40 s at 6.5 m/s). After cell disruption, the cell debris and glass beads were separated by centrifugation (5 min at 14,000 rpm). The concentration of citrate in the supernatant fluid was determined using a Citrate Assay Kit (Biovision, #K655-100). Intracellular citrate concentration was estimated according to the assumptions that the *S. aureus* cell volume is 5×10^{-13} ml (13) and that 1 A600 corresponds to 2×10^{8} cells/ml (14).

Measurement of Staphyloxanthin Production. Colonies of *S. aureus* were cultivated on TSA plate (without glucose) at 37℃ for 48 hours. Bacteria were washed from the TSA plate and subjected to methanol extraction (5). The optical density at 465 nm (OD465) was measured and normalized to the optical density (OD600) of the washed bacterial suspensions.

Siderophore Detection Assays. *S. aureus* cultures were pregrown overnight in Roswell Park Memorial Institute 1640 (RPMI) medium (Life Technologies,

#31800-022), and 1×10^7 CFU of each strain was inoculated into fresh RPMI medium. The liquid cultures were grown in a 20-ml tube with a tube volume-to-medium volume ratio of 5:1 at 37℃ with shaking for 24 hours (OD600 ≈ 2.0), 250 rpm of aeration.

Siderophore plate bioassays were performed as previously described using a chrome azurol S agar diffusion (CASAD) assay (15) with some modifications. Holes with 5-mm-diameter were punched on the CAS agar plate. Each hole was filled with 35 μl of spent culture supernatants, and the plate was incubated at 37℃ for 4-8 h. The orange halos that formed around the wells correspond to the iron-chelating activity of the siderophores.

To quantify the siderophore activity in spent culture supernatants, chrom azurol S (CAS) shuttle solution was used as previously described (9). Briefly, a 10-fold dilution of culture supernatants was mixed with equal volumes of CAS shuttle solution and incubated in darkness at room temperature for 45 mins. Absorption at 630 nm was measured using a Synergy 2 (Biotek). Siderophore units were calculated as follows: (A630 of sterile culture medium-A630 of samples)/A630 of sterile culture medium. Ultimately, siderophore units were normalized to a culture OD600 of 1.0.

Growth of *S. aureus* under Iron-limited Conditions. *S. aureus* cultures were pregrown overnight in Roswell Park Memorial Institute 1640 (RPMI) medium. The cells were washed thrice with Chelex-treated RPMI medium (iron-limited medium) (16) and each strain was inoculated into Chelex-treated RPMI medium (1×10^7

CFU/ml) with or without $FeCl_3$ (50 μM). The liquid cultures were grown in a 20-ml tube with a tube volume-to-medium volume ratio of 5:1 and shaken with 250 rpm of aeration at 37℃. Bacterial growth was monitored using a nanodrop to measure absorption at 600 nm every 3 hours for 12 hours.

Growth of *S. aureus* under iron-limited conditions was also carried out on a 96-well plate (nunc; no. 167008). Briefly, *S. aureus* cultures were pregrown overnight in RPMI. The cells were washed thrice with Chelex-treated RPMI medium. A20-μl volume of the sample containing 1×10^8 CFU of *S. aureus* bacteria was added to the wells with 180 μl Chelex-treated RPMI medium, and a 70-μl volume of filter-sterilized mineral oil was added in order to prevent evaporation during the assay. The plate was cultivated at 37℃ and absorption at 600 nm was measured every hour for 24 hours using a Synergy 2 (Biotek).

Determination of Intracellular Iron Content. *S. aureus* cultures were pregrown overnight in RPMI medium. The cells were washed thrice with RPMI and diluted into fresh RPMI medium, yielding 1×10^7 CFU/ml cultures. The liquid cultures (50 ml) were grown in 250-ml flask at 37℃ for 24 h with shaking, 250 rpm of aeration. Subsequently, the cultures were centrifuged and the cells were collected. The cell pellet was prepared and run on atomic absorption spectroscopy in order to determine intracellular iron content using PerkinElmer AA800. Final Fe concentration was displayed as a percentage on the basis of dry weight.

311 **Measuring Transferrin-Fe Release.** Overnight *S. aureus* cultures were diluted
312 100-fold in fresh TSB medium without glucose. The liquid cultures were grown in a
313 20-ml tube with a tube volume-to-medium volume ratio of 5:1, shaken at 250 rpm at
314 37℃ for 15 h. Cultures were centrifuged and supernatants were collected.
315 Measurement of the release of iron from transferrin was performed as previously
316 described (17). Iron-bound transferrin displays an absorption peak at 470 nm. When
317 iron dissociates from transferrinn, the intensity of the peak at 470 nm absorption
318 decreases. Absorption at 470 nm was measured every 1 min for 30 min upon
319 introduction of the samples. Transferrin stock solutions of 400 μM were prepared by
320 suspending human transferrin (Sigma, T8158-100) in distilled water and a final
321 concentration of transferrin at 40 μM was used for all samples. All absorption
322 readings were measured using Synergy 2 (Biotek).

323

324 **Analyses of Gene Expressions with Oligonucleotide Microarray.** Overnight
325 cultures of *S. aureus* Newman and its derivatives were washed and diluted 100-fold in
326 fresh TSB medium (without glucose) in a 20-ml tube with a tube volume-to-medium
327 volume ratio of 5:1. The liquid culture was grown at 37 ℃ for about 6 h ($OD_{600} \approx 5.0$)
328 with shaking, 250 rpm of aeration. Total RNA was immediately stabilized with
329 RNAprotect Bacteria Reagent (Qiagen, Valencia, CA) and then extracted through the
330 use of a Qiagen RNeasy kit following the manufacturer's instructions. The total
331 DNase-treated RNA samples were then analyzed by CapitalBio Corp
332 (http://www.capitalbio.com/index.asp, Beijing, China) for Chip (Affymetrix) assay.

333 Briefly, samples were labeled according to the manufacturer (Affymetrix, Santa Clara,
334 CA) and then hybridized to the Affymetrix GeneChip *S. aureus* genome array
335 (Affymetrix, Cat. no. 900514) for 16 h at 50℃ through the use of the GeneChip
336 hybridization oven at 60 rpm. Washing, staining, and scanning were performed using
337 the Affymetrix GeneChip system. The data were normalized using Robust Multi-array
338 Average (RMA) (18). Gene expression analysis was performed using three
339 independent mRNA samples for each strain. Microarray data were analyzed with
340 SAM (Significance Analysis of Microarrays) software (19). Criterion such as cutoff
341 limitation for fold change ≥2 or ≤0.5 and q-value ≤5% was used in order to select
342 differential expression genes. All data were submitted to the NCBI GEO database
343 under accession number GSE57260.

344

345 **Quantitative Real-time PCR**. The bacterial growth and the preparation of total
346 DNase-treated RNA were performed as described above. The total RNA (5 μg) was
347 reversely transcribed to synthesize cDNA using the PrimeScript RT reagent Kit
348 (Takara) with random primers. The resulting cDNA were diluted by 1:2, 1:4, and 1:8,
349 respectively. Triplicate quantitative assays were performed on 1 μl of each cDNA
350 dilution with the THUNDERBIRD™ SYBR® qPCR Mix and 300 nM primers using
351 an Applied Biosystems 7500 Fast Real-Time PCR System. Dissociation curve
352 analysis was performed in order to verify product homogeneity. The primers used for
353 Quantitative real-time PCR for *SAV1813*, *SAV1609*, *SAV1168*, *SAV1064*, *SAV1048*,

SAV0812, *SAV0423*, *SAV0149, SACOL0209,* and *SAV0114* (*sirB*) are listed in Table S2.

To measure the relative expression of *sirABC* operon when bacteria were grown in RPMI medium, *sirB* gene-specific primers were used (Table S2). *S. aureus* cultures were pregrown overnight in RPMI. The cells were washed with RPMI three times, and 1×10^7 CFU of each strain was inoculated into fresh RPMI medium. Liquid cultures were grown in 20-ml tube with a tube volume-to-medium volume ratio of 5:1 at 37 ℃ for 24 h ($OD_{600} \approx 2.0$) with shaking, 250 rpm of aeration. Total RNA was immediately stabilized with RNAprotect Bacteria Reagent (Qiagen, Valencia, CA) and then through the use of a Qiagen RNeasy kit following the manufacturer's instructions.

The amplicon of 16S rRNA was used as an internal control (20-22) in order to normalize all data. The relative quantification method (ΔΔCT) as previously described was used in order to calculate relative expression levels of interest genes (23, 24).

Construction, Expression, and Purification of the Inducer-binding Domain of $CcpE_{IBD}$. The *ccpE*$_{IBD}$ was amplified from *S. aureus* Newman genomic DNA with primers $ccpE_{IBD}$-F and $ccpE_{IBD}$-R (Table S2). The PCR product was digested with *Eco*RI and *Xho*I, and inserted into similarly cut pET28b (Novagen) in order to produce the plasmids pET28b-$ccpE_{IBD}$. DNA sequencing was used to verify the

clones, which were transformed into *E. coli* BL21 (DE3) for expression. The expression cells were grown in LB to OD600 0.6~0.8; 0.5 mM of isopropyl β-D-1-thiogalactopyranoside (IPTG) was then added. After incubation at 16 ℃ for 14~16 h, the culture was harvested, and cell pellets were resuspended in buffer A (20 mM Tris-HCl, pH 8.0; 500 mM NaCl, 0.1 mM EDTA, 10 mM 2-mercaptoethanol β-ME) and sonicated. The lysate was centrifuged at 13,000 g for 40 min, and the supernatants were loaded onto a NiNTA column (His Trap, GE Healthcare). The column was equilibrated with buffer A, and His-tagged $CcpE_{IBD}$ protein was eluted using a linear gradient of 50-400 mM imidazole. Fractions enriched for 6His-$CcpE_{IBD}$ were pooled and concentrated. The proteins were further purified on a Superdex 200 column (GE Healthcare) with buffer B (20 mM Tris-HCl, pH 8.0, 200 mM NaCl, 2 mM DTT). Selenomethionine substituted 6His-$CcpE_{IBD}$ protein was expressed using the methionine biosynthesis inhibition method (25). The expression and purification of 6His-$CcpE_{IBD}$ protein was performed as described above.

Crystallization and Structural Determination of $CcpE_{IBD}$. The 6His-$CcpE_{IBD}$ proteins and the selenomethionyl 6His-$CcpE_{IBD}$ proteins were concentrated to 12 mg/ml in buffer B (20 mM Tris-HCl, pH8.0; 200 mM NaCl, 2 mM DTT), respectively. Crystallization was performed using the hanging drop vapor diffusion method at 22 ℃. 1 μl of protein solution was mixed with 1μl of reservoir solution (0.1M Tris-HCl, pH8.5, 33% PEG3350) and equilibrated against 0.6 ml of reservoir solution. Octahedral shaped crystals appeared after a few days. Crystals were briefly

soaked in 0.1 M Tris-HCl, pH 8.5, 37% PEG3350, and cryocooled in liquid nitrogen. The diffraction data were collected at Shanghai Synchrotron Radiation Facility Beamline 17U. All of the x-ray data were processed using HKL2000 program suite (26) and converted to structural factors within the CCP4 program (27). Phasing was solved in SHELX using single wavelength anomalous dispersion data (28). A structural model was manually built in COOT (29), and computational refinement was carried out with the program REFMAC5 (30) in the CCP4 suite. Structural graphic figures were prepared in PyMOL (PyMOL Molecular Graphics System, Version 1.3 Schrödinger, DeLano Scientific LLC). Atomic coordinates and structural factors have been deposited in the Protein Data Bank (PDB, www.pdb.org) under accession ID code 4QBA.

Western Blot Analysis. *S. aureus* strains were grown at 37 ℃ overnight in tryptic soy broth (TSB) containing 10 μg/ml tetracycline. Overnight cultures of the indicated *S. aureus* strains were washed twice and diluted 100-fold in fresh TSB medium (containing 10 μg/ml tetracycline) without glucose. The liquid cultures were grown in a tube with a tube volume-to-medium volume ratio of 5:1, shaken at 250 rpm at 37 ℃ for 6 h (OD600 ≈ 5.0). 1 ml cells were harvested by centrifugation and washed with TE buffer (20 mM Tris-HCl, pH 8.0, 1 mM EDTA) and resuspended in 100 μl TE buffer. 1 μl 5mg/ml lysostaphin was added to the mixture and lysis at 37 ℃ for 3 hours. 10 μl of the pellets sample was mixed with 10 μl of 2 × SDS loading buffer (50mM Tris-HCl, pH 6.8; 2% SDS; 0.1% bromophenol blue; 1% mercaptoethanol; 10%

glycerol) and then heated at 100℃ for 15 min. SDS polyacrylamide gel electrophoresis was carried out using a 10% slab gel with a 5% stacking gel and transferred onto PVDF (Bio-Rad) membranes. PageRuler™ Prestained Protein Ladder #SM0672 (Fermentas) was used as a molecular weight reference. For detection of CcpE protein, anti-CcpE polyclonal antibody (prepared by immunizing a rabbit with a 6His-CcpE protein, Shanghai Immune Biotech CO., Ltd) and anti-rabbit IgG antibody conjugated to horseradish peroxidase (HRP) (Code#: NA934, GE Healthcare) were used. For detection of ClpP protein, anti-ClpP polyclonal antibody (12) and anti-rabbit IgG antibody conjugated to horseradish peroxidase (HRP) (Code#: NA934, GE Healthcare) were used. The chemiluminescent was detected by a Tanon-5200 multi according to the manufacturer's recommendation.

Whole-blood Killing Assays. Overnight cultures of the indicated strains were washed twice and diluted 100-fold in fresh TSB medium without glucose. The liquid cultures were grown in a 20-ml tube with a tube volume-to-medium volume ratio of 5:1, shaken at 250 rpm at 37℃ for 2 h (OD600≈0.5). 1 ml of bacterial culture was centrifuged, and staphylococci were washed and suspended in 1 ml of sterile PBS in order to generate a suspension of 1×10^7 CFU/ml. Whole blood from healthy human volunteers was collected using a BD VACUTAINER PT tube (363095). 450 μl of whole blood was transferred into a 20-ml tube and mixed with 50 μl bacterial sample, which resulted in 1×10^6 CFU/ml. The tubes were incubated at 37℃ for 5 h with shaking (180 rpm), at which time dilutions were plated on a TSA agar plate for

enumeration of surviving CFU.

Mouse Infection Model. Since we observed that *S. aureus* Newman loses plasmid pYJ335 during infection, we used Newman/pCL-lacZ strain (wild-type Newman strain harbors a single-site integration vector pCL-lacZ), Δ*ccpE*/pCL-lacZ strain (Δ*ccpE* mutant harbors a single-site integration vector pCL-lacZ), and the complementary strain Δ*ccpE*/pCL-*ccpE* (Δ*ccpE* mutant harbors a single-site integration vector pCL-*ccpE*) to determine the effect of *ccpE* deletion on the virulence of *S. aureus* Newman strain.

An ca. 1.7 kb DNA fragment containing the *ccpE* gene and the tetracycline-inducible *xyl*/*tetO* promoter of pYJ335 were PCR amplified from p-*ccpE* DNA with primers ccpE-pCL-F (with *Eco*RI site) and ccpE-pCL-R (with *Kpn*I site) (Table S2). The resulting PCR products were cut with the restriction enzymes *Eco*RI and *Kpn*I and ligated with plasmid pCL-LacZ that had been cut with the same enzymes, generating pCL-*ccpE* (Table S1). The pCL-*ccpE* plasmid was electroporated into the *S. aureus* strain RN4220 and then transformed into mutants using bacteriophage Ø85. As a control, the empty pCL-LacZ vector (8) was integrated into the chromosomes of Newman and Δ*ccpE* through the use of a similar method. Overnight cultures in TSB medium (without glucose) of the indicated strains were washed and diluted 100-fold in fresh TSB medium (without glucose) in a 20-ml tube with a flask volume-to-medium volume ratio of 5:1. The liquid culture was grown at

37℃ for about 3 h with shaking (OD600 ≈3), 250 rpm of aeration, and then the bacteria were harvested and washed twice with ice-cold, phosphate-buffered saline. The CFU (Colony-Forming-Units) per milliliter were determined before mice were inoculated.

Mouse infections were carried out as described previously (2, 5) with some modifications, using 8-week-old female BALB/c mice obtained from Shanghai SLAC Laboratory Animal Co. Ltd. and housed under specified pathogen-free conditions. All animal experiments were reviewed and approved by the Institutional Animal Care and Use Committee (IACUC) of the Shanghai Public Health Clinical Center and were performed in accordance with the relevant guidelines and regulations. Mice were anaesthetized with pentobarbital sodium (intraperitoneal injection, 80 mg/kg) and were infected retro-orbitally with ca. 3×10^6 cfu of each bacterial isolate. Animals were sacrificed 5 days post infection. Kidneys and livers were aseptically removed and homogenized in PBS plus 0.1% Triton X-100 to obtain single-cell suspensions. Serial dilutions of each organ were plated on TSA (Difco) plates for the enumeration of CFU.

Table S1. Plasmids and strains used in this study

Strains or plasmids	Relevant genotype or characteristic	Source
Plasmids		
pKOR1	Gene replacement vector for *S. aureus* genes, Amp^r, Cm^r	(1)
pYJ335	*E. coli-S. aureus* shuttle vector, Cm^r , Erm^r	(6)
pCL-lacZ	*E.coli-S. aureus* shuttle cloning vector, single-copy integration vector in *S.*	(8)

	aureus; pCL55 carrying promoterless *lacZ*; Cm^r in *S. aureus*	
pET28a	Km^r, expression vector	Novagen
pET28b	Km^r, expression vector	Novagen
pAT18	A plasmid containing an *ermB* gene	(4)
pT181	A tetracycline-resistance plasmid from *S. aureus*	(7)
pYJ335-Tc	pYJ335 carrying a 1.6 kb tetracycline resistance cassette from plasmid pT181	This study
pET28a::*ccpE*	pET28a derivative carrying *ccpE* (*NWMN_0641*) of *S. aureus* Newman	This study
pET28a::$ccpE_{R145A}$	pET28a::*ccpE* carrying alanine substitution mutant at the site arginine 145 of CcpE	This study
pET28a::$ccpE_{R256A}$	pET28a::*ccpE* carrying alanine substitution mutant at the site arginine 256 of CcpE	This study
p-*ccpE*	pYJ335 derivative carrying *ccpE* (*NWMN_0641*) in the downstream of the *xyl/tet* promoter region	This study
pT-*ccpE*	Plasmid pYJ335-Tc carrying CcpE	This study
pT-$ccpE_{R145A}$	pT-*ccpE* carrying alanine substitution mutant at the site arginine 145 of CcpE	This study
pT-$ccpE_{R256A}$	pT-*ccpE* carrying alanine substitution mutant at the site arginine 256 of CcpE	This study
p-*citB*	pYJ335 carrying *citB* (*NWMN_1263*) in the downstream of the *xyl/tet* promoter region	This study
pKOR1::Δ*ccpE*	pKOR1 derivative, for deletion of *ccpE* gene	This study
pKOR1::Δ*citB*	pKOR1 derivative, for deletion of *citB* gene	This study
pCL-*citB-lacZ*	pCL-lacZ derivative carrying *citB* (NWMN_1263) promoter	This study
pCL-*cap5A-lacZ*	pCL-lacZ derivative carrying *cap5A* (NWMN_0095) promoter	This study
pCL-*SAV1168-lacZ*	pCL-lacZ derivative carrying NWMN_1077 (*SAV1168* in *S. aureus* Mu50) promoter	This study
pCL-*citB-M-lacZ*	pCL-*citB-lacZ* derivative carrying *citB* promoter with mutations in the CcpE binding site	This study
pCL-*SAV1168-M-lacZ*	pCL-*SAV1168-lacZ* derivative carrying	This study

	SAV1168 promoter with mutations in the CcpE binding site	
pCL-*crtO-lacZ*	pCL-lacZ derivative carrying *crtO* promoter	This study
pCL::*ccpE*	pCL-lacZ derivative carrying *ccpE* (*NWMN_0641*) gene	This study
Strains		
Newman	Wild-type, *S. aureus* ATCC 25904	(31)
JE2	*S. aureus* LAC cured of all 3 native plasmids; Erm^s	(32)
RN4220	Derivative of 8325-4 that accepts plasmids	(33)
Δ*ccpE*	*ccpE* gene deletion mutant of Newman strain	This study
Δ*citB*	*citB* gene deletion mutant of Newman strain	This study
Δ*ccpE*Δ*citB*	*ccpE* and *citB* double gene deletion mutant of Newman strain	This study
JE2-Δ*ccpE*	*ccpE* deletion mutant of JE2 strain; transduced from Δ*ccpE*. Erm^r	This study
JE2-*citB*	*citB* insertion mutant (NE861) of JE2 strain	(32)
Newman::pCL-lacZ	*S. aureus* Newman carrying an empty integration vector pCL-lacZ	This study
Newman::*citB-lacZ*	*S. aureus* Newman carrying an integration vector pCL-*citB-lacZ*	This study
Newman::*SAV1168-lacZ*	*S. aureus* Newman carrying an integration vector pCL-*SAV1168-lacZ*	This study
Newman::*cap5A-lacZ*	*S. aureus* Newman carrying an integration vector pCL-*cap5A-lacZ*	This study
Δ*ccpE*::pCL-lacZ	Δ*ccpE* strain carrying an integration vector pCL-lacZ	This study
Δ*ccpE*::*citB-lacZ*	Δ*ccpE* strain carrying an integration vector pCL-*citB-lacZ*	This study
Δ*ccpE*::*SAV1168-lacZ*	Δ*ccpE* strain carrying an integration vector pCL-*SAV1168-lacZ*	This study
Δ*ccpE*::*cap5A-lacZ*	Δ*ccpE* strain carrying an integration vector pCL-*cap5A-lacZ*	This study
Δ*ccpE*::pCL-*ccpE* (Δ*ccpE-C*)	Δ*ccpE* strain carrying an integration vector pCL-*ccpE*	This study
Newman::*citB-M-lacZ*	*S. aureus* Newman carrying an integration vector pCL-*citB-M-lacZ*	This study
Δ*ccpE*::*citB-M-lacZ*	Δ*ccpE* strain carrying an integration	This study

	vector pCL-*citB-M-lacZ*	
Δ*ccpE*Δ*citB*::*citB-lacZ*	Δ*ccpE*Δ*citB* strain carrying an integration vector pCL-*citB-lacZ*	This study
Δ*ccpE*Δ*citB*::*SAV1168-lacZ*	Δ*ccpE*Δ*citB* strain carrying an integration vector pCL-*SAV1168-lacZ*	This study
Δ*ccpE*Δ*citB*::*cap5A-lacZ*	Δ*ccpE*Δ*citB* strain an integration vector pCL-*cap5A-lacZ*	This study
Δ*citB*::*citB-lacZ*	Δ*citB* strain carrying an integration vector pCL-*citB-lacZ*	This study
Δ*citB*::*SAV1168-lacZ*	Δ*citB* strain carrying an integration vector pCL-*SAV1168-lacZ*	This study
Δ*citB*::*cap5A-lacZ*	Δ*citB* strain carrying an integration vector pCL-*cap5A-lacZ*	This study
JE2::*citB-lacZ*	JE2 carrying an integration vector pCL-*citB-lacZ*	This study
JE2::*SAV1168-lacZ*	JE2 carrying an integration vector pCL-*SAV1168-lacZ*	This study
JE2-Δ*ccpE*::*citB-lacZ*	JE2-Δ*ccpE* strain carrying an integration vector pCL-*citB-lacZ*	This study
JE2-Δ*ccpE*::*SAV1168-lacZ*	JE2-Δ*ccpE* strain carrying an integration vector pCL-*SAV1168-lacZ*	This study
Newman/pYJ335	Newman strain carrying plasmid pYJ335	This study
Δ*ccpE*/pYJ335	Δ*ccpE* strain carrying plasmid pYJ335	This study
Δ*ccpE*/p-*ccpE*	Δ*ccpE* strain carrying p-*ccpE*	This study
Δ*ccpE*/p-*citB*	Δ*ccpE* strain carrying p-*citB*	This study
Δ*citB*/pYJ335	Δ*citB* strain carrying plasmid pYJ335	This study
Δ*citB*/p-*citB*	Δ*citB* strain carrying plasmid p-*citB*	This study
Newman::*citB-lacZ*/pYJ335-Tc	Newman::*citB-lacZ* carrying plasmid pYJ335-Tc	This study
Δ*ccpE*::*citB-lacZ*/pYJ335-Tc	Δ*ccpE*::*citB-lacZ* carrying plasmid pYJ335-Tc	This study
Δ*ccpE*::*citB-lacZ*/pT-*ccpE*	Δ*ccpE*::*citB-lacZ* carrying plasmid pT-*ccpE*	This study
Δ*ccpE*::*citB-lacZ*/pT-$ccpE_{R145A}$	Δ*ccpE*::*citB-lacZ* carrying plasmid pT-$ccpE_{R145A}$	This study
Δ*ccpE*::*citB-lacZ*/pT-$ccpE_{R256A}$	Δ*ccpE*::*citB-lacZ* carrying plasmid pT-$ccpE_{R256A}$	This study
JE2/pYJ335	JE2 carrying plasmid pYJ335	This study
JE2-Δ*ccpE*/pYJ335	JE2-Δ*ccpE* carrying plasmid pYJ335	This study
JE2-*citB*/pYJ335	JE2-*citB* carrying plasmid pYJ335	This study
JE2-*citB*/p-*citB*	JE2-*citB* carrying plasmid p-*citB*	This study
JE2-Δ*ccpE*/p-*ccpE*	JE2-Δ*ccpE* carrying plasmid p-*ccpE*	This study

E. coli		
BL21(DE3)	F^- *ompT hsdS*$_B$ (r_B^- m_B^-) *gal dcm met* (DE3)	Laboratory stock
DH5α	*endA hsdR17 supE44 thi-1 recA1 gyrA relA1*Δ(*lacZYA-argF*)*U169 deoR* (*φ80dlac*Δ(*lacZ*)*M15*)	Laboratory stock

482 Amp^r, ampicillin resistance; Kan^r, kanamycin resistance; Cm^r, chloroamphenicol
483 resistance; Erm^r, erythromycin resistance; Tet^r, tetracycline resistance

484

485

486 **Table S2. Primers used in this study.**

Primers	Sequence (5′to 3′)
ccpE-up-F	GCCGGATCCTGAAGGTGGTTTCTAT
ccpE-up-R	CGCGAAGCTTAGTCTTCAATCTTCATA
ccpE-down-F	CGCAAGCTTAAAAGTAGAAATTGAT
ccpE-down-R	GGCCCCTCGAGAACCTATACTTACT
erm-F	GGGCAAGCTTAGCCATGACTTTTTTAG
erm-R	GGGAAGCTTTCTCCATTCCCTTTAGTAAC
ccpE-BP-F	GGGGACAAGTTTGTACAAAAAAGCAGGCTTGAAGGTG GTTTCTATAGAGAGA
ccpE-BP-R	GGGGACCACTTTGTACAAGAAAGCTGGGTAAGCCAAC CCATAATACTAAAA
citB-up-F	GGAATTCCATATGATCTGTATTTGCGACAATCGT
citB-up-R	CGCGGATCCATTTAATGATCCCCCTTGATA
citB-down-F	CGCGGATCCCTCGTGACTGGGCAGCAAAAG
citB-down-R	CCGCTCGAGGATTGGCTCGCTTATCATTCA
citB-BP-F	GGGGACAAGTTTGTACAAAAAAGCAGGCTGGAATTCCA TATGATCTGTATTTGCGACAATCGT
citB-BP-R	GGGGACCACTTTGTACAAGAAAGCTGGGTCCGCTCGAG GATTGGCTCGCTTATCATTCA
ccpE-F	AATAATTGAATAATTTATGGGGGGAAATT
ccpE-R	CTACGCCTTTGGTTGTTCAACAA
ccpE-R-tet	CCCGAATTCCTACGCCTTTGGTTGTTCAACAA
tet-F	CCCGAATTCAATCGATTTTTGGCAACA
tet-R	AAATGCTAGCCACTCATAGTTC
citB-F	ACCTAAATTAAGCGTTTTCTAAG
citB-R	ACTATCAAAGTGCCTCAAATACCGA
SAV1609-F	CAATCACCACCCAGTCATCAAC (For qRT-PCR)

SAV1609-R	AAGTATTTAGCAGCGAGCGTGA (For qRT-PCR)
SAV1168-F	TGTCCACCGATGATAGTTTGTTGT (For qRT-PCR)
SAV1168-R	GTTTGGCATAGTCATTTTCAAGTGT (For qRT-PCR)
SAV1064-F	AACAAGTAGTATCCGCACATCGT (For qRT-PCR)
SAV1064-R	TACCTCCTGGCATTTGAACAAT (For qRT-PCR)
SAV1048-F	ATTTTTCCTTTACTTTCCGACATTG (For qRT-PCR)
SAV1048-R	TTATCCAAATGGTGGTTTCACTGCT (For qRT-PCR)
SAV0812-F	CAACAACGCATCAATCACCTAC (For qRT-PCR)
SAV0812-R	GTTCACGCTTGATTACACGCTTC (For qRT-PCR)
SAV0423-F	TGGTCTTTACGGTGAAATGAGT (For qRT-PCR)
SAV1813-F	ATTCTATCTTTCGCTTTTGCTCCTT (For qRT-PCR)
SAV1813-R	ATTCAGTGGTAGTATTTGCGGGTG (For qRT-PCR)
SAV0423-R	ATAACATCGGACATACGGTCTTCT (For qRT-PCR)
SAV0149-F	AAGGGTGACAATCCTCAGTTTA (For qRT-PCR)
SAV0149-R	CCGAATCTCGTTTATGACCACTT (For qRT-PCR)
SACOL0209-F	GCTCATCTAAACTTGAACTAAAACC (For qRT-PCR)
SACOL0209-R	ATGGCTTATTGAATCTTGGTCT (For qRT-PCR)
sirB-F	GATAAGACCCACAAAGACG (For qRT-PCR)
sirB-R	GATTATTCCGCTTGTATTG (For qRT-PCR)
16sRNA-F	CGTGGAGGGTCATTGGA (For qRT-PCR)
16sRNA-R	CGTTTACGGCGTGGACTA (For qRT-PCR)
ccpE-PF	GGGGGATCCATGAAGATTGAAGACTA
ccpE-PR	CCGACTCGAGTCTAAAACTACGCCT
$ccpE_{IBD}$-F	CCGGAATTCGATGATTATTGAGCATGCCCGTGAC
$ccpE_{IBD}$-R	CCGCTCGAGCTACGCCTTTGGTTGTTCAACAAAG
R145AF	GATTATCATGTTATGATAACTGCCGGAAATAAGGTAATG
R145AR	AAATTCATTACCTTATTTCCGGCAGTTATCATAACATG
R256AF	GAACCGCTGATTGCCTCGACATTTATGAGTTATGATC
R256AR	TCATAAATGTCGAGGCAATCAGCGGTTCATTATCAATTTC
ccpE-pCL-F	GGGAATTCCTTGGTTACCGTGAAGTTACCATCACGG
ccpE-pCL-R	CGGGGTACCCTACGCCTTTGGTTGTTCAACAA
lacZ0149-F	CTAAGAATTCAGAAGCACTAATCAGTG
lacZ0149-R	TAAGGTACCGATTGTCACCCTTAG
lacZ1350-F	ATTAAACTACGAATTCTCGATTTTT
lacZ1350-R	CCGGGTACCTTTTAAATCATAGTAAG
lacZ1168-F	GTTAATAAGAATTCTACCTCTTGTC
lacZ1168-R	CCGGGTACCTTGATTAACTCATTGATATTAGTCTCGT
citB-M-F	TATAAGCAAAGTGGCGCATACAGGTAAGGTGTAATAA
citB-M-R	CCTTACCTGTATGCGCCACTTTGCTTATATACTCTGA
1350FAM	FAM-CTTCTACAGCTTTTAAATCATAGTAAG
1168FAM	FAM-TTGATTAACTCATTGATATTAGTCTCGT
cap-p-F	ACAATCATTTTTTTAAATAAAGAA

cap-p-R	TTTGATTCACTAAGATTTGAG
1168-p-F	TTGATTAACTCATTGATATTAGTCTCGT
1168-p-R	TTTCTGTCCAAAACTTAAAAATGAT
citB-p-F	CCGGAATTCATAATTATTCTCAATTA
citB-p-R	CTTCTACAGCTTTTAAATCATAGTAAG
citB-pB-F	TGTATGATAAGTTTTGCTTATATACTCTGATTAAAAAGTC AAAACCT
citB-pM-F	TGTATGCGCCACTTTGCTTATATACTCTGATTAAAAAGTC AAAACCT
ccpE-cF	GTTACACAAAGACTAAAAGCTATTG
ccpE-cR	GTAACTTTGTAACATCATCTCG
citB-pc-F	CCGGAATTCACTCTGATTAAAAAGTCAA
citB-12F	ATCATTTCTGTCCCACTCCCATC
citB-12R	GTAAGTATAACTTTGGCCATTCAAGTC
1168M1F	CTTAAACAGTTAGTAGTGTTATGGCCATAAAACT TATCATTT
1168M1R	AAACTTAAAAATGATAAGTTTTATGGCCATAACACTACT AA
lacZ-crtO-F	AACGAATTCCACTTGGACAGGAAATTGGAA
lacZ-crtO-R	AAAGGTACCTGGTTTTCATCTAAATTGAATCACT

Table S3. Data collection and refinement statistics of SeMet-substituted $CcpE_{IBD}$ crystal [a]

	Se-$CcpE_{IBD}$ (4QBA)
Data collection	
Space group	P 21 21 21
Cell dimensions	
a, *b*, *c* (Å)	73.60, 77.18, 93.97
α, β, γ (°)	90, 90, 90
Resolution (Å)	50.0-2.20 (2.28-2.20)[b]
No. of observations	379242
No. unique	51385 (5157)
R_{sym} [c]	0.071 (0.485)
$I/\sigma(I)$	20.0 (3.7)
Completeness (%)	99.4 (100)
Redundancy	7.4 (7.6)
Data refinement	
Resolution (Å)	30.0-2.21 (2.26-2.21)
No. reflections	25824 (1791)
R_{work}/R_{free}	20.2/24.3
No. atoms	

Protein	3226
Ligand	2
Solvent	67
B factors (Å^2)	54.7
Rmsd[d] in	
Bond lengths (Å)	0.008
Bond angles ( )	1.291
Ramachandran Plot[e]	
Favored (%)	98.0
Accepted (%)	1.8
Outliers (%)	0.2

[a]Each structure was solved using one crystal.

[b]Highest resolution shell is shown in parenthesis.

[c]$R_{sym} = \Sigma|(I - <I>)|/\Sigma(I)$, where I is the observed intensity.

[d]Root mean squared deviation.

[e]Values calculated in CCP4 suite using Procheck.

Table S4. 55 genes whose expressions are down-regulated more than 2-fold in Δ*ccpE* strain compared to the wild-type Newman strain

Gene	Fold change*	Target description	Biological process
SAV1168	0.11	Superantigen-like protein	Pathogenesis
SAV1167	0.13	Superantigen-like protein	Pathogenesis
SAV1166	0.15	Superantigen-like protein	Pathogenesis
SAV0814	0.15	Extracellular matrix binding protein	Pathogenesis
SACOL0859	0.19	Extracellular matrix and plasma binding protein	Pathogenesis
SAV0812	0.20	Secreted von Willebrand factor-binding protein	Pathogenesis
SAV0426	0.21	Superantigen-like protein Set11	Pathogenesis
SACOL0857	0.24	Staphylocoagulase precursor	Pathogenesis
SAV0423	0.24	Superantigen-like protein Set7	Pathogenesis
SA1755	0.29	Chemotaxis-inhibiting protein CHIPS	Pathogenesis
SAV0428	0.29	Superantigen-like protein Set13	Pathogenesis
SAV1156	0.31	Formyl peptide receptor-like 1 inhibitory protein	Pathogenesis
SAV0813	0.31	Extracellular ECM and plasma binding protein Ssp	Pathogenesis
SAV0427	0.32	Superantigen-like protein Set12	Pathogenesis

SAV0429	0.33	Superantigen-like protein Set14	Pathogenesis
SAV0229	0.33	Complement inhibitor	Pathogenesis
SAV2503	0.35	Fibronectin-binding protein FnbA	Pathogenesis
SA0385	0.36	Superantigen-like protein Set9	Pathogenesis
SAV0424	0.37	Superantigen-like protein Set8	Pathogenesis
SACOL0209	0.37	Staphylocoagulase precursor	Pathogenesis
SAV0370	0.42	Enterotoxin	Pathogenesis
SAV0425	0.44	Superantigen-like protein Set10	Pathogenesis
SAV2502	0.46	Fibronectin-binding protein FnbB	Pathogenesis
SAV1604	0.12	Transmembrane transport protein	Transport
SAV2438	0.17	Amino acid ABC transporter	Transport
SAV0736	0.37	Iron complex transport system substrate-binding protein	Transport
SA0325	0.43	Glycerol-3-phosphate transporter	Transport
SAV0115	0.45	Iron(III) ABC transporter SirA	Transport
SAV2352	0.47	Multidrug resistance protein	Transport
SAV0114	0.48	Iron(III) ABC transporter SirB	Transport
SAV1607	0.10	Acetyl-CoA carboxylase biotin carboxyl carrier protein subunit	Metabolic process
SAV1606	0.11	Acetyl-CoA carboxylase	Metabolic process
SAV1608	0.14	Putative urea carboxylase	Metabolic process
SAV1350	0.16	Aconitate hydratase CitB	Metabolic process
SAV1609	0.18	Urea carboxylase	Metabolic process
SAV0984	0.49	3-oxoacyl-ACP synthase	Metabolic process
SAV0672	0.04	Transcriptional regulator CcpE	Regulation of transcription
SAV0518	0.38	GntR family transcriptional regulator	Regulation of transcription
SAV0698	0.38	Transcription repressor of fructose operon	Regulation of transcription
SAV2357	0.40	TcaR transcription regulator	Regulation of transcription
SAV1273	0.27	30S ribosomal protein S15	Translation
SAV0539	0.37	50S ribosomal protein L10	Translation
SAV1605	0.12	LamB/YcsF family protein	Unclassified
SAV0579	0.43	VraX	Unclassified
SAV0023	0.44	5'-nucleotidase	Unclassified
SAV1638	0.26	Hypothetical protein	Hypothetical protein
SAV0371	0.29	Hypothetical protein	Hypothetical protein
SAV2556	0.30	Hypothetical protein	Hypothetical protein

SAV0220	0.35	Hypothetical protein	Hypothetical protein
SACOL0479	0.38	Hypothetical protein	Hypothetical protein
SAV2611	0.44	Hypothetical protein	Hypothetical protein
SAV1036	0.45	Hypothetical protein	Hypothetical protein
SAV1421	0.47	Hypothetical protein	Hypothetical protein
SAV2592	0.48	Hypothetical protein	Hypothetical protein
SAV0373	0.48	Hypothetical protein	Hypothetical protein

[a] Genes are referenced with *S. aureus* strain Mu50, COL, or N315. *Microarray data were analyzed with SAM (Significance Analysis of Microarrays) software. The criterion of cutoff limitation as a fold change ≥2 or ≤0.5 and q-value ≤5% was used in order to select differential expression genes.

Table S5. 71 genes whose expressions are up-regulated more than 2-fold in Δ*ccpE* strain compared to the wild-type Newman strain

Gene[a]	Fold change*	Target description	Biological Process
SAV0152	10.03	Capsular polysaccharide synthesis enzyme Cap5D	Pathogenesis
SAV0151	9.24	Capsular polysaccharide synthesis enzyme Cap8C	Pathogenesis
SAV0150	8.90	Capsular polysaccharide synthesis enzyme Cap5B	Pathogenesis
SAV0149	8.49	Capsular polysaccharide synthesis enzyme Cap5A	Pathogenesis
SAV0154	8.35	Capsular polysaccharide synthesis enzyme Cap5F	Pathogenesis
SAV0156	8.09	Capsular polysaccharide synthesis enzyme Cap5H	Pathogenesis
SAV0153	7.95	Capsular polysaccharide synthesis enzyme Cap8E	Pathogenesis
SAV0155	7.70	Capsular polysaccharide synthesis enzyme Cap5G	Pathogenesis

SAV0163	6.49	Capsular polysaccharide synthesis enzyme Cap8O	Pathogenesis
SAV0160	6.16	Capsular polysaccharide synthesis enzyme Cap5L	Pathogenesis
SAV0157	6.11	Capsular polysaccharide synthesis enzyme Cap5I	Pathogenesis
SAV0159	5.90	Capsular polysaccharide synthesis enzyme Cap5K	Pathogenesis
SAV0162	5.88	Capsular polysaccharide synthesis enzyme Cap5N	Pathogenesis
SAV0164	5.80	Capsular polysaccharide synthesis enzyme Cap5P	Pathogenesis
SAV0161	5.35	Capsular polysaccharide synthesis enzyme Cap5M	Pathogenesis
SAV0158	5.11	Capsular polysaccharide synthesis enzyme Cap5J	Pathogenesis
SACOL1865	4.40	Serine protease SplE	Pathogenesis
SAV1809	4.24	Serine protease SplF	Pathogenesis
SAV1813	3.97	Serine protease SplA	Pathogenesis
SAV1812	3.61	Serine protease SplB	Pathogenesis
SAV1048	3.21	Serine protease SspA	Pathogenesis
SAV1909	3.02	Cysteine protease Staphopain A	Pathogenesis
SAV0815	2.89	Nuclease Nuc	Pathogenesis
SAV1047	2.87	Cysteine protease SspB	Pathogenesis
SAV2654	2.84	Serine-threoinine rich antigen	Pathogenesis
SAV2637	2.49	Zinc metalloproteinase aureolysin	Pathogenesis
SAV2638	2.21	Immunodominant antigen B	Pathogenesis
SAV2388	2.68	Nitrite extrusion protein	Transport
SAV2653	2.38	Preprotein translocase subunit SecY	Transport
SAV1933	2.36	ABC transporter ATP-binding protein	Transport
SAV2415	2.31	Multidrug resistance protein YcnB	Transport
SAV0383	2.18	Proton/sodium-glutamate symport protein	Transport
SAV1816	2.18	Lantibiotic ABC transporter protein	Transport
SAV0103	2.15	Major facilitator transporter	Transport
SAV1931	2.07	ABC transporter ATP-binding protein	Transport
SAV1068	4.99	Phosphoribosylformylglycinamidine synthase I PurQ	Purine biosynthesis
SAV1064	4.98	Phosphoribosylaminoimidazole	Purine

		carboxylase	biosynthesis
SAV1067	4.76	Phosphoribosylformylglycinamidine synthase PurS	Purine biosynthesis
SAV1066	4.70	Phosphoribosylaminoimidazole-succinocarboxamide synthase PurC	Purine biosynthesis
SAV1069	4.01	phosphoribosylformylglycinamidine synthase II PurL	Purine biosynthesis
SAV1065	3.83	Phosphoribosylaminoimidazole carboxylase ATPase subunit PurK	Purine biosynthesis
SAV0095	3.21	1-phosphatidylinositol phosphodiesterase precurosr	Metabolic process
SAV0177	2.83	Formate dehydrogenase	Metabolic process
SAV1114	2.39	Pyruvate carboxylase	Metabolic process
SAV1026	3.59	Competence transcription factor	Regulation of transcription
SACOL1871	2.05	Epidermin immunity protein F	Unclassified
SAV2096	2.01	ssDNA-binding protein	Unclassified
SAV0808	4.89	Hypothetical protein	Hypothetical protein
SAV2205	4.05	Hypothetical protein	Hypothetical protein
SACOL0850	3.82	Hypothetical protein	Hypothetical protein
SAV0170	3.41	Hypothetical protein	Hypothetical protein
SACOL1870	2.85	Hypothetical protein	Hypothetical protein
SAV0807	2.81	Hypothetical protein	Hypothetical protein
SAV0596	2.72	Hypothetical protein	Hypothetical protein
SACOL0643	2.63	Hypothetical protein	Hypothetical protein
SACOL2202	2.56	Hypothetical protein	Hypothetical protein
SACOL1532	2.53	Hypothetical protein	Hypothetical protein
SACOL1533	2.50	Hypothetical protein	Hypothetical protein
SAV2543	2.37	Hypothetical protein	Hypothetical protein

SAV2342	2.31	Hypothetical protein	Hypothetical protein
SACOL0486	2.30	Hypothetical protein	Hypothetical protein
SAV2587	2.29	Hypothetical protein	Hypothetical protein
SAV2492	2.28	Hypothetical protein	Hypothetical protein
SACOL2201	2.27	Hypothetical protein	Hypothetical protein
SAV0289	2.20	Hypothetical protein	Hypothetical protein
SAV0740	2.18	Hypothetical protein	Hypothetical protein
SAV2474	2.17	Hypothetical protein	Hypothetical protein
SAV0859	2.14	Hypothetical protein	Hypothetical protein
SACOL2205	2.11	Hypothetical protein	Hypothetical protein
SAV0297	2.07	Hypothetical protein	Hypothetical protein
SAV0447	2.02	Hypothetical protein	Hypothetical protein

[a] Genes are referenced with *S. aureus* strain Mu50 or COL. *Microarray data were analyzed with SAM (Significance Analysis of Microarrays) software. The criterion of cutoff limitation as a fold change ≥2 or ≤0.5 and q-value ≤5% was used in order to select differential expression genes.

Table S6. Verification of microarray results by Real-Time RT-PCR[a]

Gene	Target description	Microarray	qRT-PCR
SAV0149	Capsular polysaccharide synthesis enzyme Cap5A	8.49	6.43
SAV1168	Superantigen-like protein	0.11	0.14
SAV1048	Serine protease SspA	3.21	3.22

SAV0812	Secreted von Willebrand factor-binding protein	0.20	0.44
SAV1609	Urea carboxylase	0.18	0.20
SAV0423	Superantigen-like protein Set7	0.24	0.59
SAV1813	Serine protease SplA	3.97	2.83
SAV1064	Phosphoribosylaminoimidazole carboxylase	4.98	2.01
SACOL0209	Staphylocoagulase precursor	0.37	0.51
SAV0114	Iron(III) ABC transporter SirB	0.48	0.47
SAV0114	Iron(III) ABC transporter SirB	N/A	0.17[b]

[a]The primers used for Real-Time RT-PCR are listed in Table S2. [b]Total RNAs were prepared from *S. aureus* growth in RPMI medium. Relative expression levels (fold change, ΔccpE *vs* wild-type Newman) of interest genes were calculated with the relative quantification method (ΔΔCT) as described in Experimental Procedures. N/A, Not Applicable.

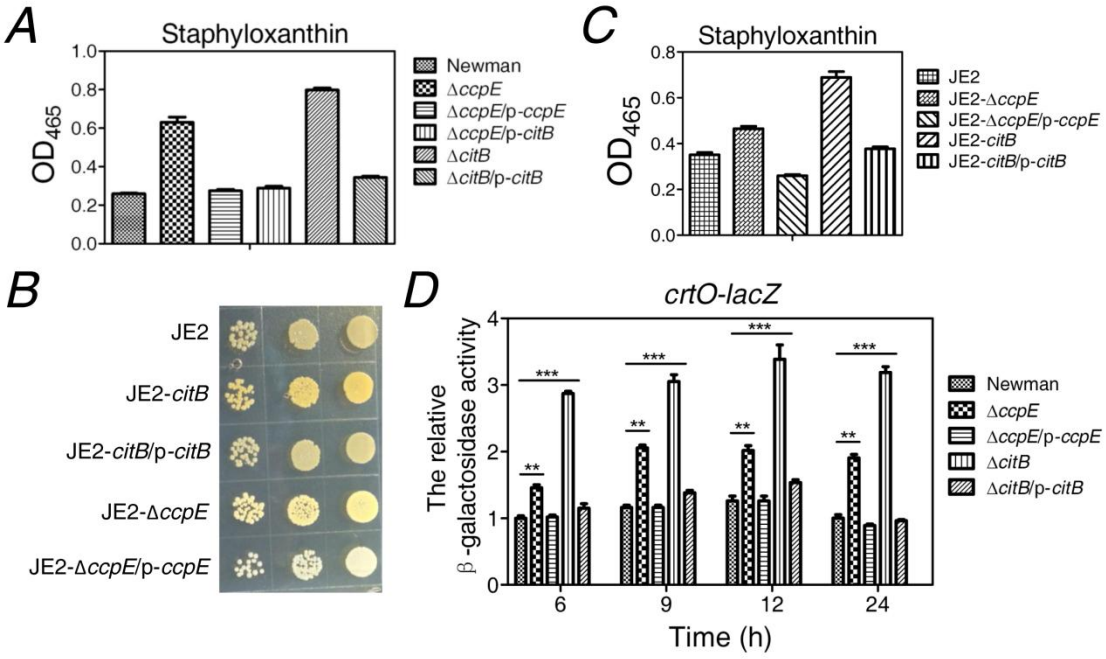

Fig. S1. Staphyloxanthin production of *S. aureus* and the promoter activity of *crtOPQMN* operon. (***A***) Staphyloxanthin production of *S. aureus* wild-type Newman strain and its derivatives, as indicated. (***B***) Pigmentation of *S. aureus* JE2 strain and its derivatives grown on TSA plates at 37 ℃ for 24 h is shown. (***C***) Staphyloxanthin production by *S. aureus* wild-type JE2 strain and its derivatives. (***D***) The absence of either *ccpE* or *citB* results in an increase of *crtO-lacZ* activity when bacteria are grown in TSB medium without glucose. Values are relative to wild-type Newman bacteria that were grown for 6 hours (set to 1). ** $p<0.01$, *** $p<0.001$ (*t*-test). In all panels, Newman, Δ*ccpE*, Δ*citB*, JE2, JE2-Δ*ccpE*, and JE2-Δ*citB* harbor plasmid pYJ335, respectively. Bacteria were grown on a TSA plate at 37 ℃ for 24 h and the staphyloxanthin production of different *S. aureus* strains was measured by methanol extraction. Relative optical density units at 465 nm were normalized to the optical density (OD600) of the washed bacterial suspensions. Results are means ± standard error of the means (errors bars) reflecting experiments conducted in triplicate.

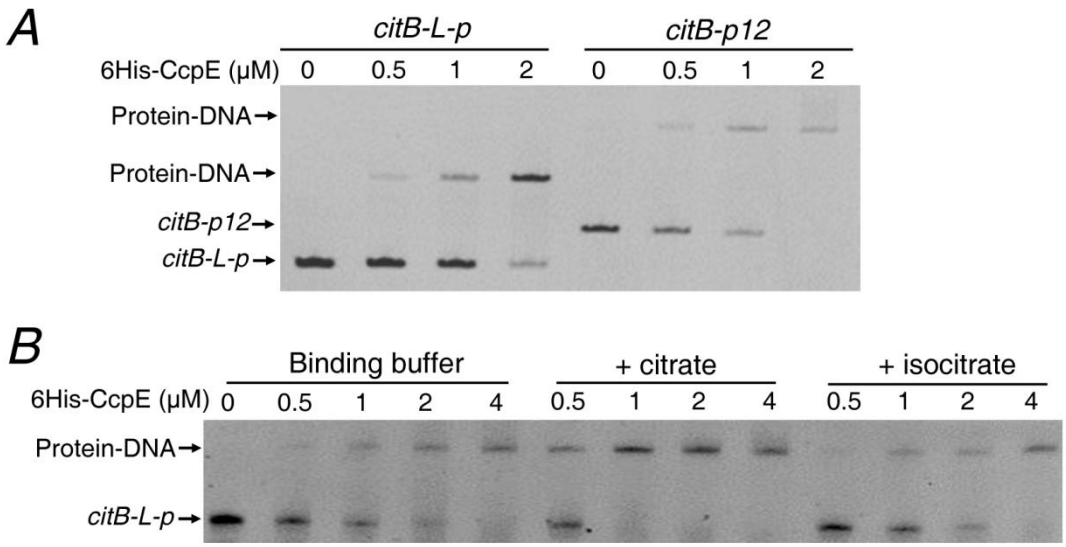

Fig. S2. (***A***) EMSA showing that *citB-p12* DNA fragment has higher affinity for 6His-CcpE than *citB-L-p* in the absence of citrate. *citB-p12*, a DNA fragment (from −321 to +66 of the start codon of *citB*) covering both the CcpE-protected regions I and II. *citB-L-p*, a DNA fragment (from −194 to +88 of the start codon of *citB*) covering the CcpE-protected region I but not II. (***B***) EMSA showing that sodium citrate (10 mM) but not sodium isocitrate (10 mM) enhances the binding of 6His-CcpE to a DNA fragment (*citB-L-p*) of *citB* promoter.

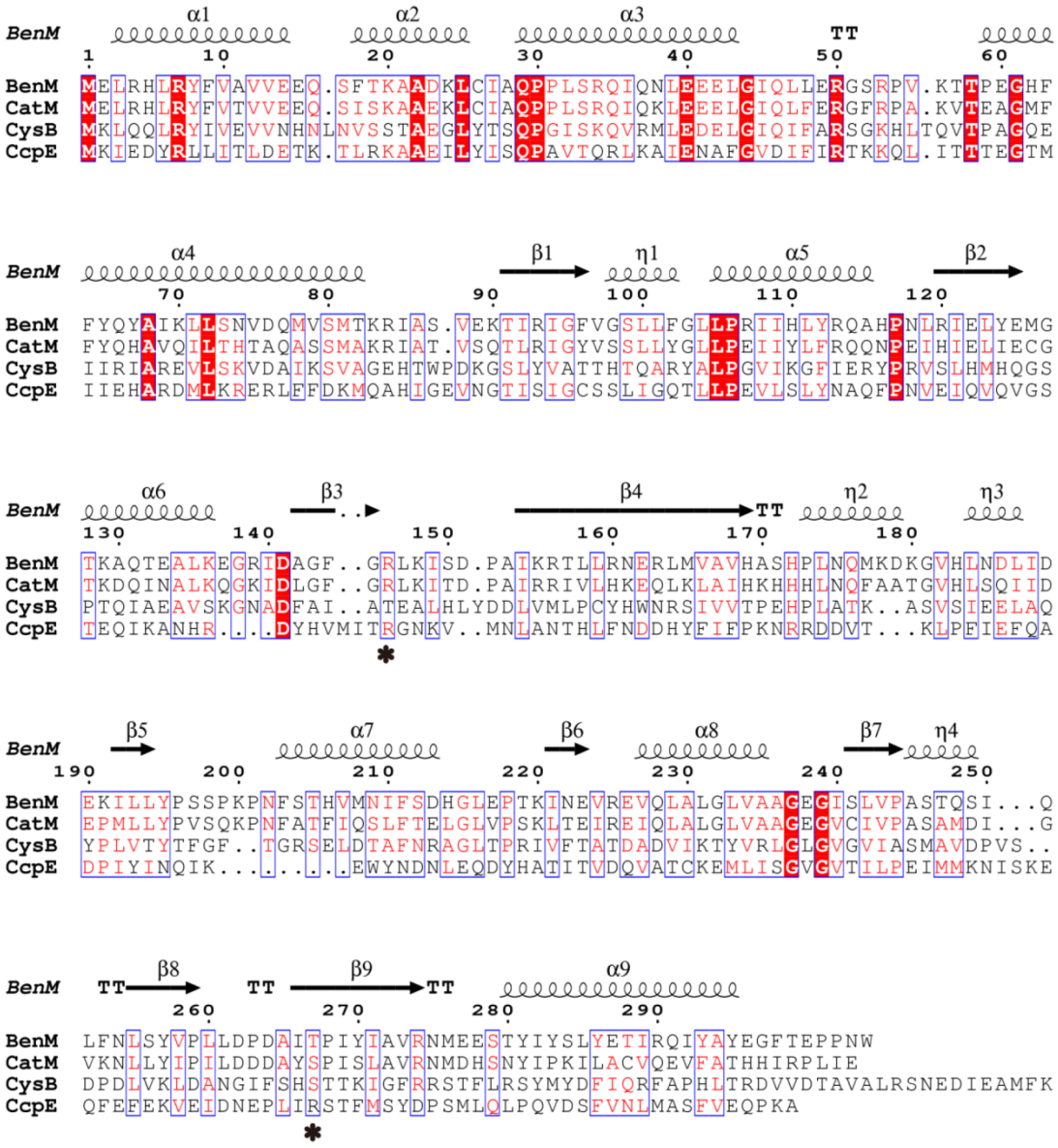

Fig. S3. Sequence alignment and secondary structure assignment of LTTRs. Structure-based sequence alignment of CcpE to BenM (PDB code 2F6G), CatM (PDB code 2F7B), and CysB (PDB code 1AL3) was performed in EXPRESSO (3DCoffee) (34), and CcpE was manually aligned according to the crystal structure. Figure was drawn with ESPript (35). The red background is intended to highlight identical residues; residues in red font are highly homologous. An asterisk is used below to mark two arginine residues (Arg145 and Arg256) located in the putative inducer-binding cavity (IBC) of CcpE. Secondary structure elements presented in the

full-length BenM structure (PDB code 3K1N) are shown on top of the sequence alignment, with residue numbers depicted at top of the alignment following BenM.

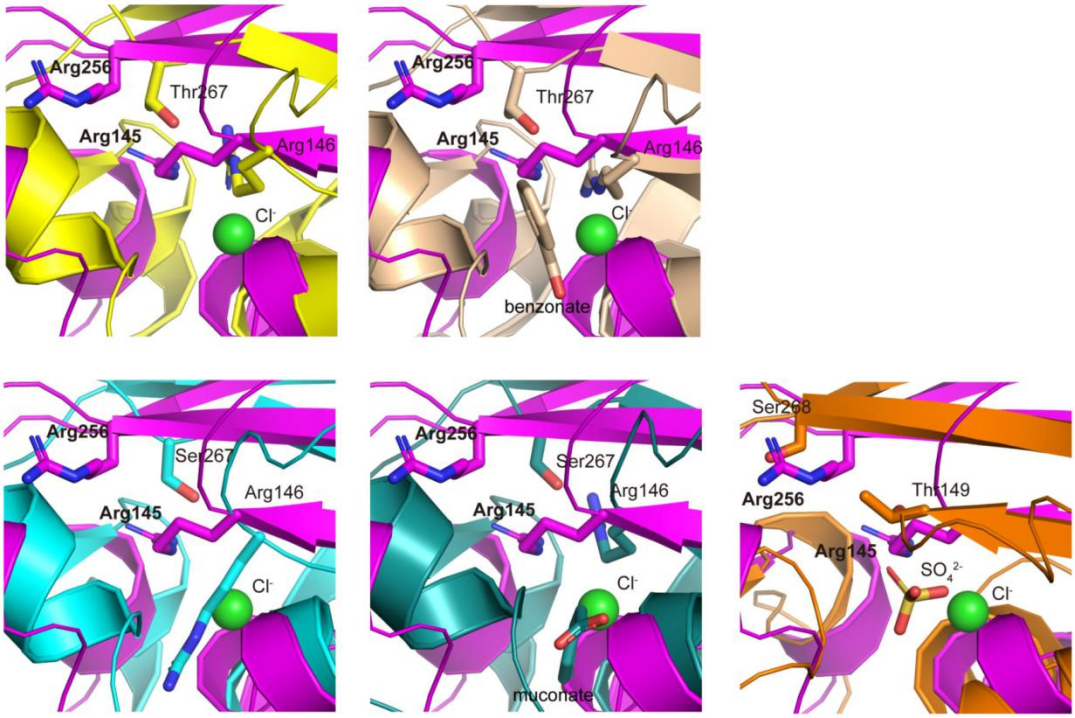

Fig. S4. Close view and comparison of the putative inducer-binding cavity (IBC) of LysR transcriptional regulators. The crystal structures of BenM (PDB code 2F6G in yellow), BenM/benzonate (PDB code 2F78 in wheat), CatM (PDB code 2F7B in cyan), CatM/muconate (PDB code 2F7C in deepteal), and CysB (PDB code 1AL3 in orange) were individually aligned to the structure of CcpE (PDB code 4QBA in magenta) in PyMoL, respectively. The same view was extracted and presented in order to show the putative inducer-binding cavity for each LysR protein. The two residues Arg145 and Arg256 are shown as sticks in CcpE, and the sequence and secondary structure correspondence residues in other LysR members are labeled. The inducers (benzonate or muconate) are shown and colored in the same mode to protein.

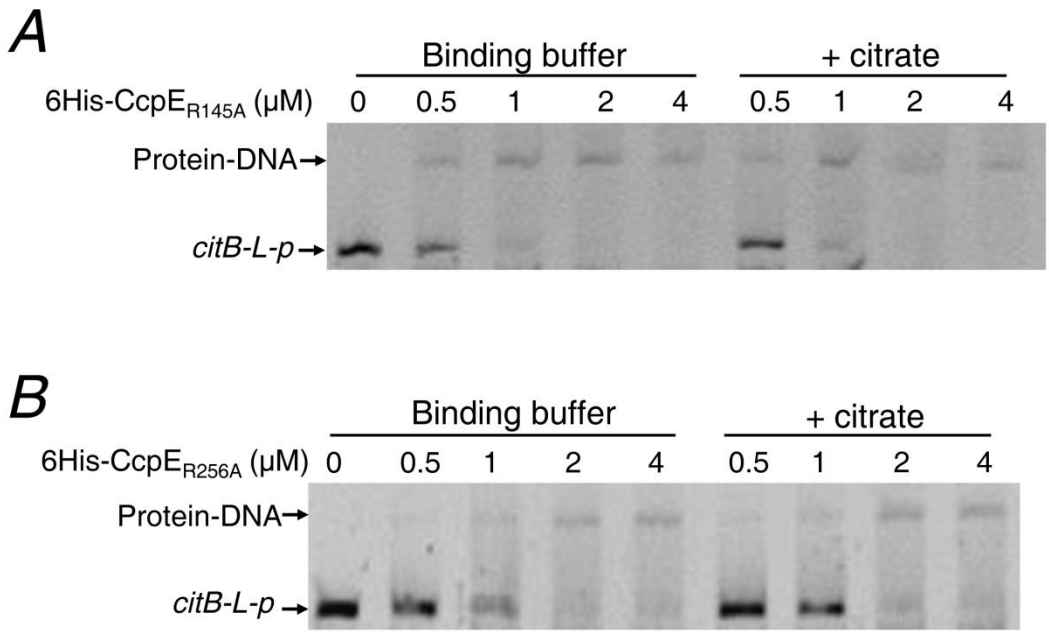

Fig. S5. EMSA showing that sodium citrate (10 mM) fails to enhance the binding of either 6His-CcpE$_{R145A}$ (***A***) or 6His-CcpE$_{R256A}$ (***B***) to a promoter DNA fragment of *citB*. *citB-L-p*, a 282 bp DNA fragment covering the CcpE-protected region I of the promoter region of *citB* (from -194 to +88 of the start codon).

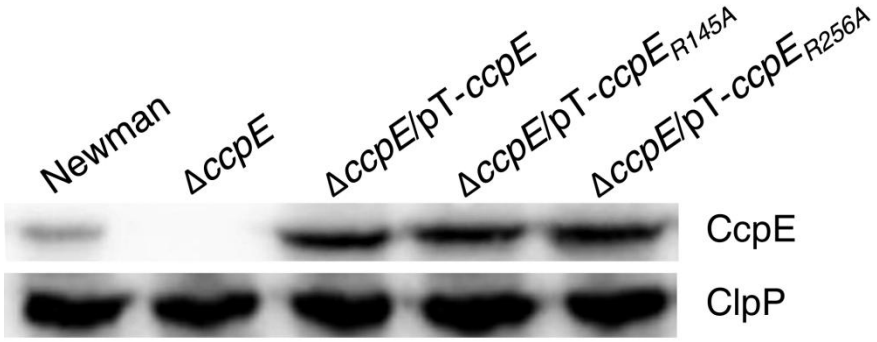

Fig. S6. Western blot analysis showing that missense mutations in *ccpE* do not affect protein levels of CcpE. Immunoblots for ClpP served as loading control. Wild-type Newman and Δ*ccpE* strain harbor the control plasmid pYJ335-Tc, respectively. Cell lysates were used as described in the experimental procedures section.

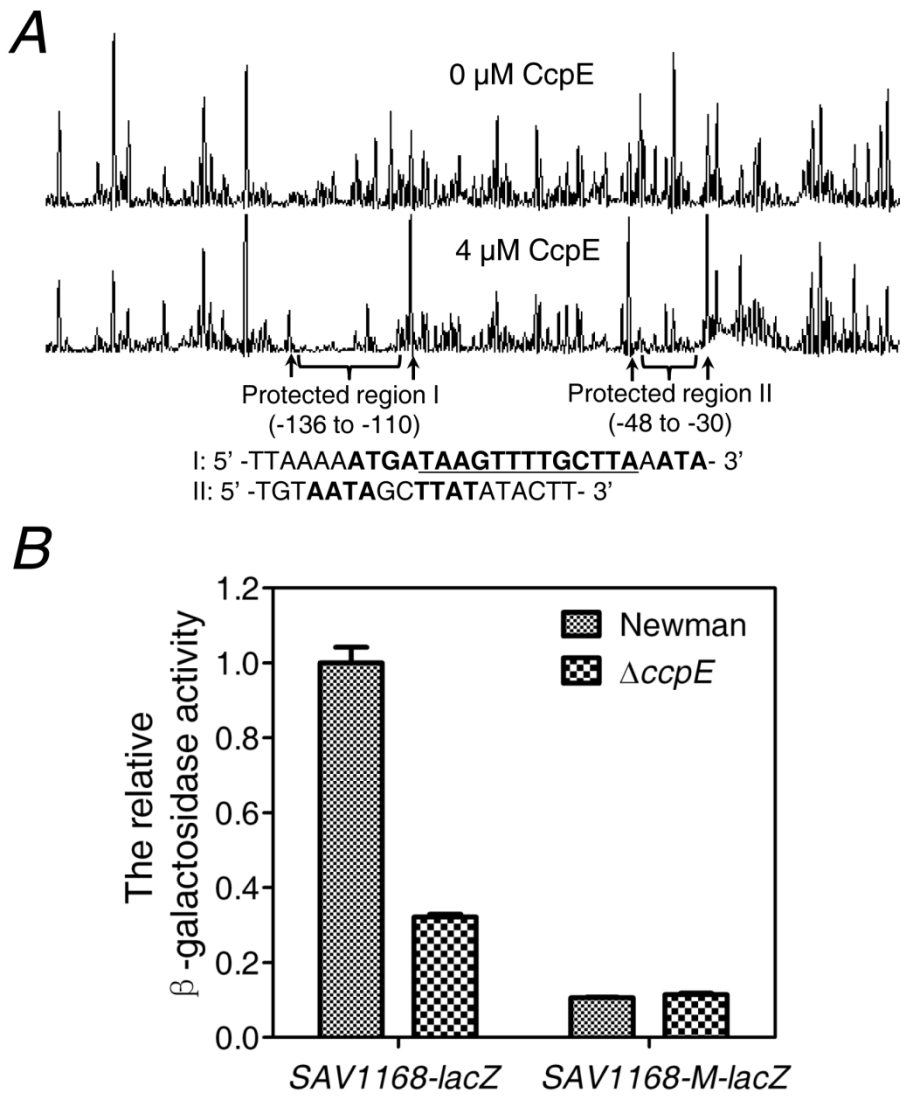

Fig. S7. (***A***) Electropherograms show the protection pattern of the *NWMN_1077* promoter after digestion with DNase I following incubation in the absence or the presence of 6His-CcpE (4 μM). Protection is seen throughout the region from -136 to -30 and there are two apparent CcpE-protected regions (I and II) in the promoter of *NWMN_1077*. The DNA sequences of the two CcpE-protected regions are illustrated. Arrows indicate DNase I-hypersensitive sites (-137, -106, -50, and -28) at the edges of the protected regions. Protected regions I: the potential LTTR box is underlined and similar DNA sequences between the protected regions I of *SAV1168* and *citB* are in bold. Protected regions II: the two box II-like sequences (AATA and TTAT) are in

bold letters. (***B***) Effects of mutations on the protected region I on the promoter activity of *SAV1168*. *SAV1168-lacZ*, a promoter-*lacZ* reporter fusion with *SAV1168* promoter DNA (from -511 to +158 of the start codon of *SAV1168*) was cloned into pCL-lacZ as described in the experimental procedures section. ATGATAAGTTTTGCTTAAATA of *SAV1168* promoter was mutated to ATGATAAGTTTTATGGCCATA**,** yielding *SAV1168-M-lacZ*. Bacteria were grown in TSB at 37℃ with shaking, 250 rpm of aeration, and sampled at 6 h. Values are relative to wild-type Newman (set to 1). Results represent means ± SEM and data are representative of three independent experiments.

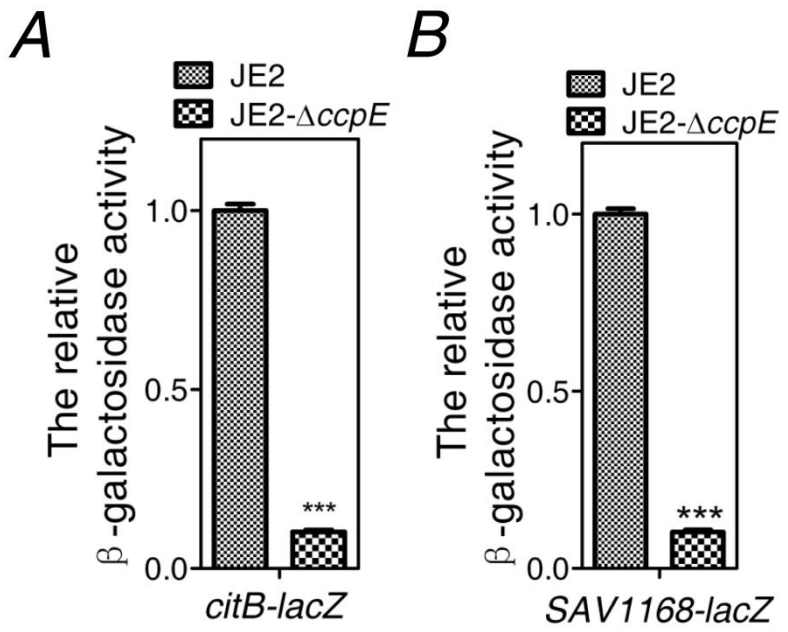

646

647 **Fig. S8.** The expression of either *citB-lacZ* (***A***) and *SAV1168-lacZ* (***B***) in JE2 strain
648 and JE2-Δ*ccpE* strain. *S. aureus* was grown in TSB at 37 ℃ with shaking, 250 rpm of
649 aeration, and sampled at 6 h. Values are relative to wild-type JE2 strain (set to 1),
650 respectively. Results represent means ± SEM and data are representative of three
651 independent experiments. *** $p<0.001$ (*t*-test).

652

653

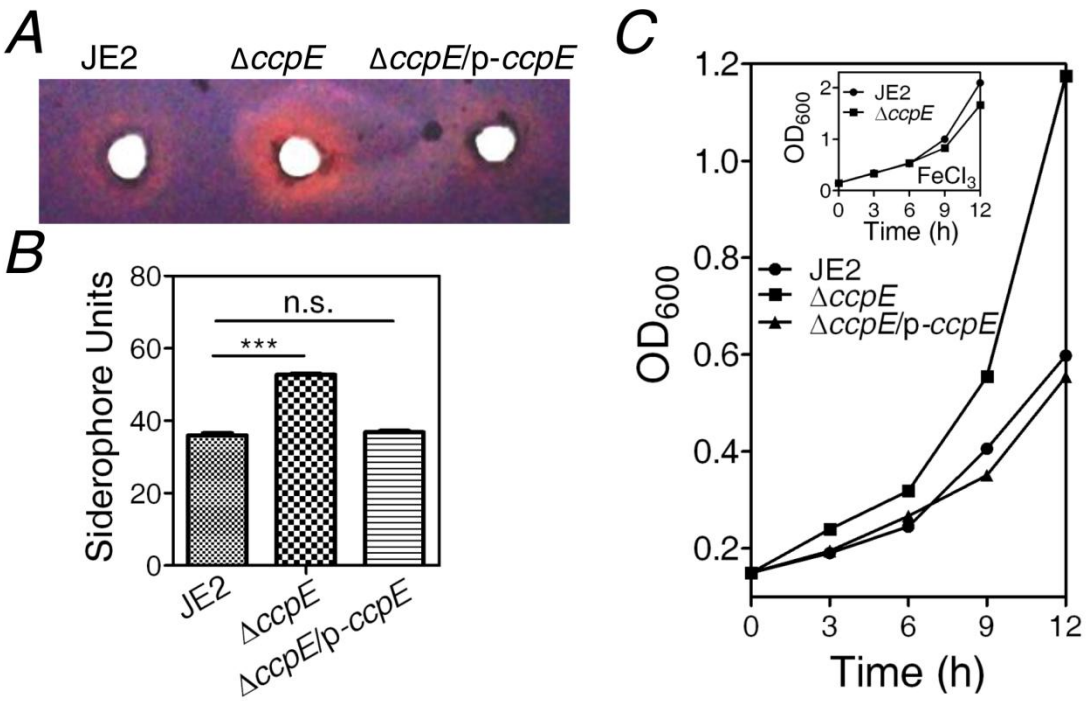

654

655 **Fig. S9.** Deletion of *ccpE* results in improved ability of the *S. aureus* JE2 strain to
656 acquire iron. In all panels, wild-type JE2 and its isogenic *ccpE* deletion mutant
657 (JE2-Δ*ccpE*, showing as Δ*ccpE* in this Figure) harbor plasmid pYJ335, respectively.
658 (***A***) Assessment of the siderophore production using a chrome azurol S agar diffusion
659 (CASAD) assay as described in the Experimental procedure. The orange halos formed
660 around the wells correspond to the iron-chelating activity of the siderophores. (***B***)
661 Siderophore levels in spent culture supernatants of wild-type JE2 strain and its
662 derivatives, as indicated. Siderophore units were calculated as described in
663 Experimental procedures. Values represent means ± SEM. (***C***) Representative growth
664 curves for *S. aureus* grown in iron-limited and in iron-sufficient medium (inserts).
665 Data are representative of three independent experiments.

666

667

668

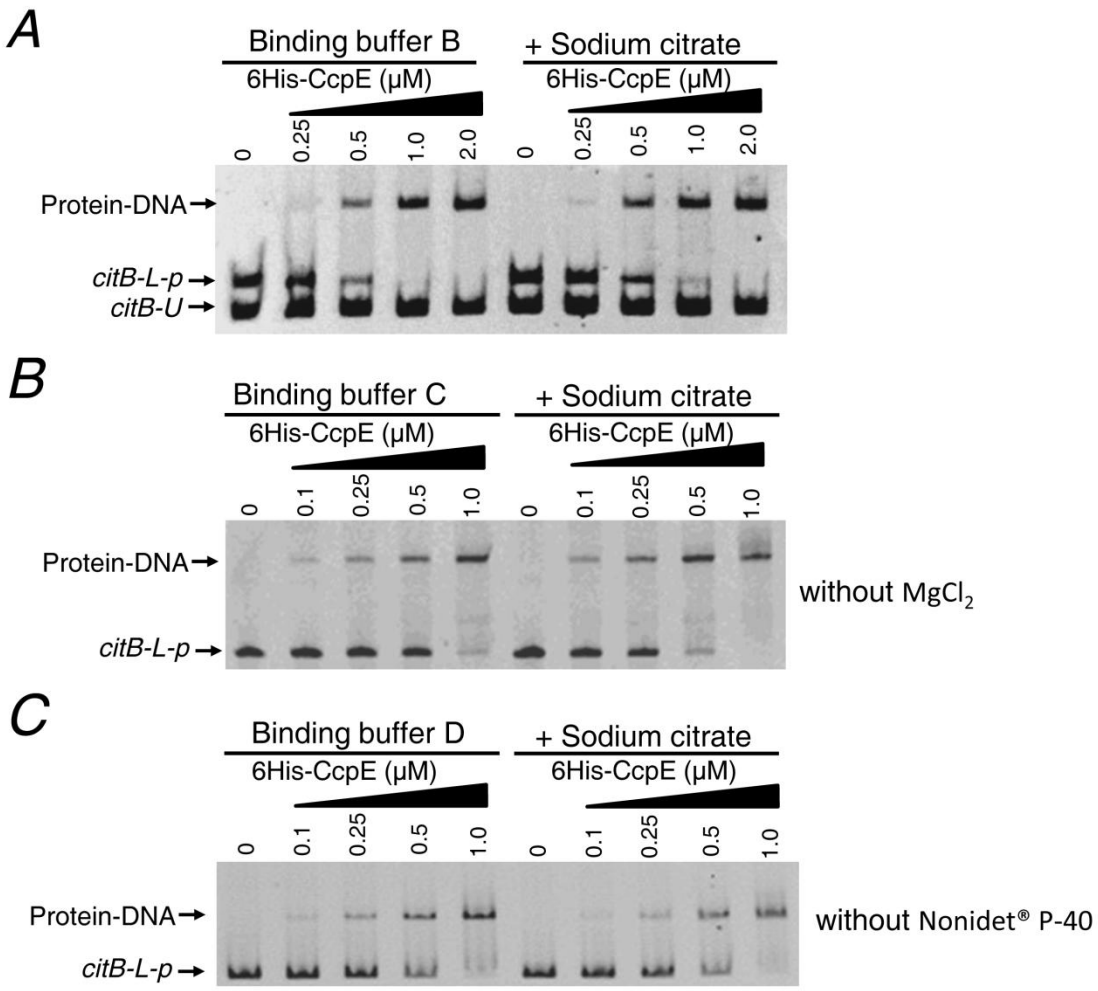

669

670 **Fig. S10.** (***A***) EMSA showing that sodium citrate (10 mM) fails to increase the
671 DNA-binding ability of 6His-CcpE to a promoter DNA fragment of *citB* (*citB-L-p*) in
672 binding buffer B [10mM Tris-HCl, pH 7.5; 50 mM NaCl, 1mM EDTA, 1mM DTT,
673 and 5% Glycerol] (36). (***B***) EMSA showing that sodium citrate (10 mM) is able to
674 increase the DNA-binding ability of 6His-CcpE in binding buffer C [20mM Tris-HCl,
675 pH 7.4; 50 mM KCl, 1 mM EDTA, 5% Nonidet® P-40, and 5% Glycerol] (Mg^{2+} was
676 eliminated from binding buffer A described in the Experimental procedure, termed
677 binding buffer C). (***C***) EMSA showing that sodium citrate (10 mM) fails to increase
678 the DNA-binding ability of 6His-CcpE in binding buffer D [20mM Tris-HCl, pH 7.4;
679 50 mM KCl, 20 mM $MgCl_2$, 1 mM EDTA, and 5% Glycerol] (Nonidet® P-40 was

680 eliminated from binding buffer A, termed binding buffer D). *citB-L-p*, a 282 bp DNA
681 fragment covering the CcpE-protected region I of the promoter region of *citB* (from
682 -194 to +88 of the start codon). *citB-U*, a DNA fragment of *citB* promoter DNA (from
683 -128 to +88 of the start codon of *citB*) containing no CcpE-protected region.
684
685
686
687
688
689
690
691
692

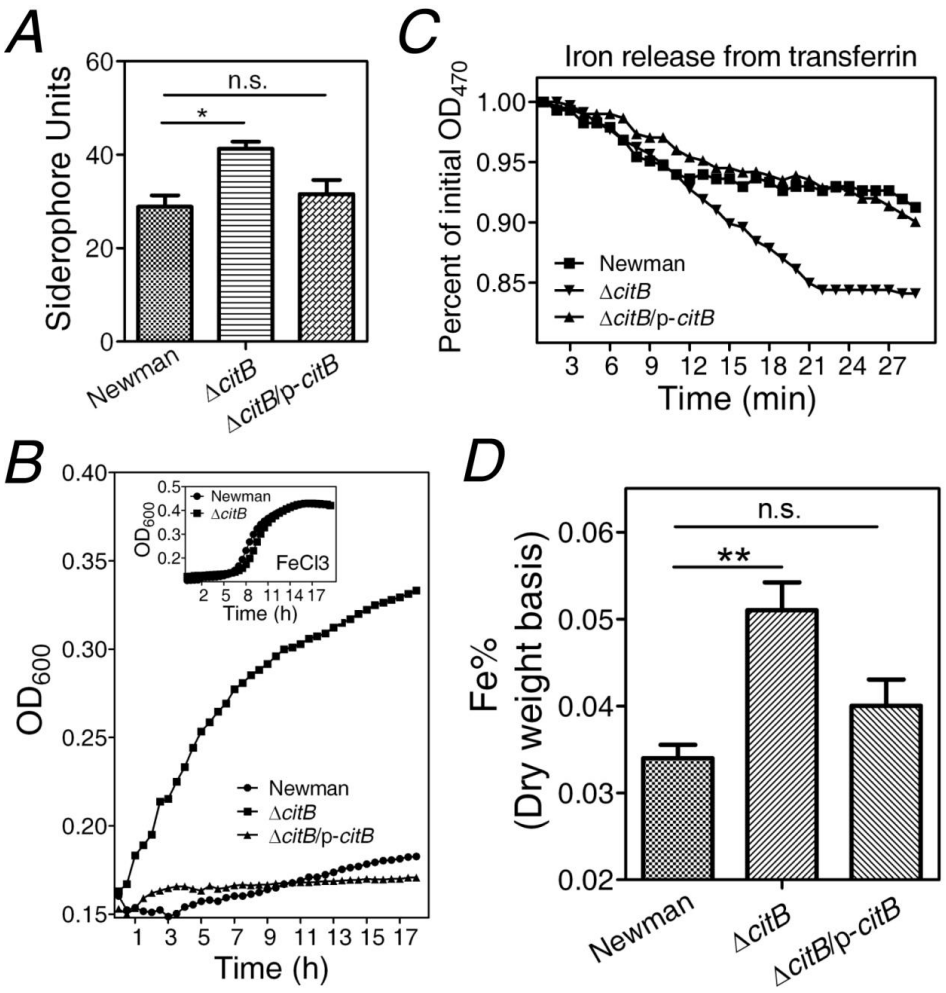

693

694 **Fig. S11.** Deletion of *citB* results in improved ability of *S. aureus* to acquire iron. In
695 all panels, wild-type Newman and Δ*citB* strain harbor plasmid pYJ335, respectively.
696 (***A***) Siderophore levels in spent culture supernatants of Newman strain and its
697 derivatives, as indicated. Siderophore units were calculated as described in
698 Experimental procedures. (***B***) Representative growth curves for *S. aureus* grown in
699 iron-limited and in iron-sufficient medium (inserts). Data are representative of three
700 independent experiments. (***C***) Iron release from transferrin mediated by various spent
701 medium from wild-type Newman strain and its derivatives, as indicated. A decrease in
702 optical density signifies a release of iron from transferrin. Data are representative of
703 three independent experiments. (***D***) Determination of intracellular iron content of

wild-type Newman strain and its derivatives, as indicated. Bacteria were grown in RPMI medium for 24 h with shaking, 250 rpm of aeration. After that, cells were collected, prepared for and run on atomic absorption spectroscopy. Results for iron content as a percentage of the dry weight. Values represent means ± SEM and data are representative of three independent experiments. The statistical difference was determined by unpaired two-tailed Student's t-test and asterisks denote statistical significance: *$p < 0.05$; **$p < 0.01$; n.s., not significant.

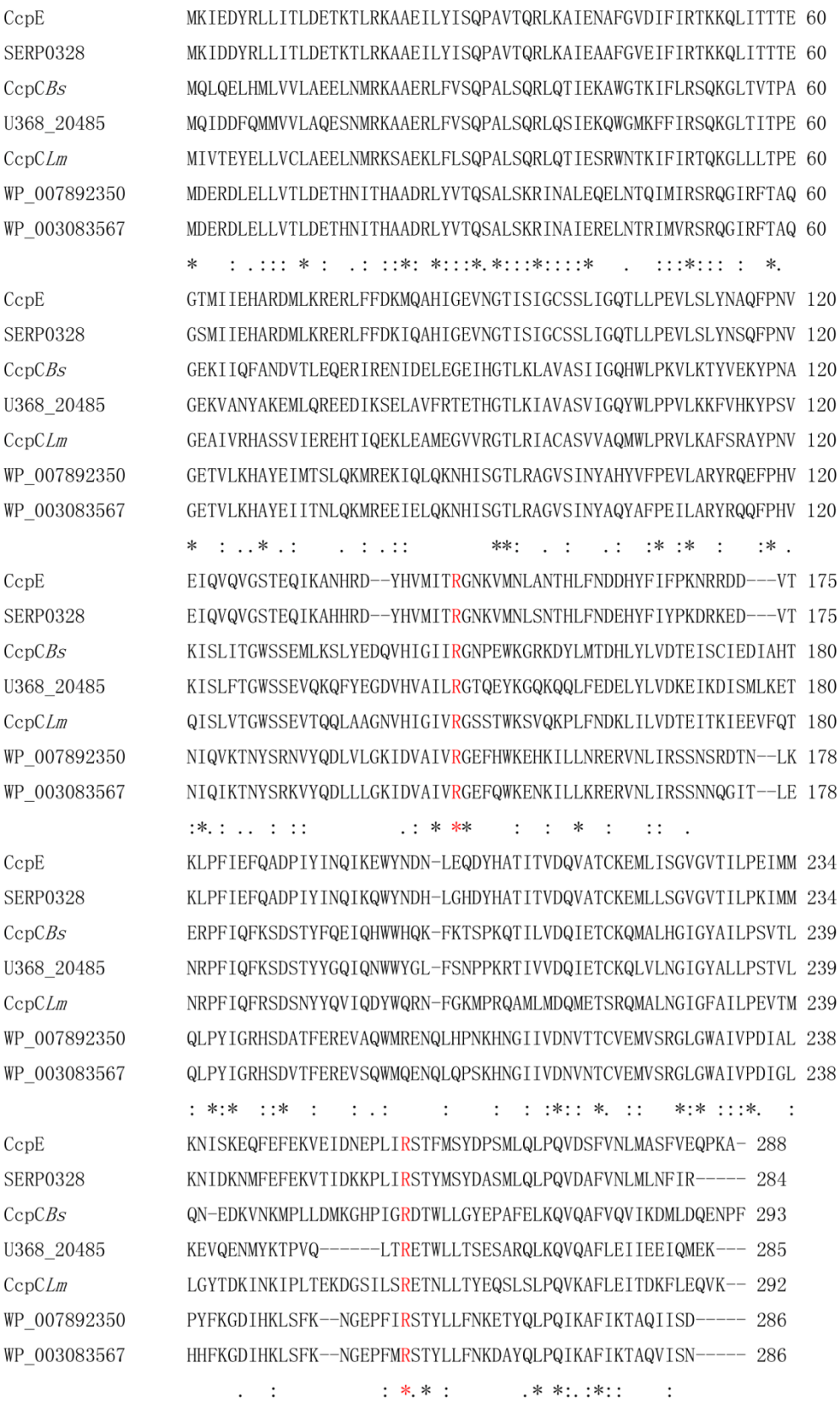

716

717 **Fig. S12.** Sequence alignment of CcpE homologues in *Staphylococcus epidermidis*

718 (SERP0328), *Bacillus subtilis* (CcpC*Bs*), *Bacillus anthracis* (U368_20485), *Listeria*

monocytogenes (CcpC*Lm*), *Streptococcus pseudoporcinus* (WP_007892350), and *Streptococcus porcinus* (WP_003083567). The different sequences were aligned using the ClustalW program. The two conserved arginine residues (Arg256 and Arg145) are in red. Stars indicate identical amino acids, double dots (:) indicate conserved amino acids, and single dots (.) indicate that residues are more or less similar.

References

1. Bae T & Schneewind O (2006) Allelic replacement in Staphylococcus aureus with inducible counter-selection. *Plasmid* 55(1):58-63.
2. Sun F*, et al.* (2012) Protein cysteine phosphorylation of SarA/MgrA family transcriptional regulators mediates bacterial virulence and antibiotic resistance. *Proceedings of the National Academy of Sciences of the United States of America* 109(38):15461-15466.
3. Liu X*, et al.* (2013) Oxidation-sensing regulator AbfR regulates oxidative stress responses, bacterial aggregation, and biofilm formation in Staphylococcus epidermidis. *The Journal of biological chemistry* 288(6):3739-3752.
4. Trieu-Cuot P, Carlier C, Poyart-Salmeron C, & Courvalin P (1991) Shuttle vectors containing a multiple cloning site and a lacZ alpha gene for conjugal transfer of DNA from Escherichia coli to gram-positive bacteria. *Gene* 102(1):99-104.
5. Lan L, Cheng A, Dunman PM, Missiakas D, & He C (2010) Golden pigment production and virulence gene expression are affected by metabolisms in Staphylococcus aureus. *Journal of bacteriology* 192(12):3068-3077.
6. Ji Y, Marra A, Rosenberg M, & Woodnutt G (1999) Regulated antisense RNA eliminates alpha-toxin virulence in Staphylococcus aureus infection. *Journal of bacteriology* 181(21):6585-6590.
7. Khan SA & Novick RP (1983) Complete nucleotide sequence of pT181, a tetracycline-resistance plasmid from Staphylococcus aureus. *Plasmid* 10(3):251-259.
8. Sun F*, et al.* (2010) In the Staphylococcus aureus two-component system sae, the response regulator SaeR binds to a direct repeat sequence and DNA binding requires phosphorylation by the sensor kinase SaeS. *Journal of bacteriology* 192(8):2111-2127.
9. Deng X*, et al.* (2012) Expression of multidrug resistance efflux pump gene norA is iron responsive in Staphylococcus aureus. *Journal of bacteriology* 194(7):1753-1762.
10. Chen B*, et al.* (2012) Development of cell-active N6-methyladenosine RNA demethylase FTO inhibitor. *Journal of the American Chemical Society* 134(43):17963-17971.
11. Zianni M, Tessanne K, Merighi M, Laguna R, & Tabita FR (2006) Identification of the DNA bases of a DNase I footprint by the use of dye primer sequencing on an automated capillary DNA analysis instrument. *Journal of biomolecular techniques : JBT* 17(2):103-113.

12. Cao Q*, et al.* (2014) A Novel Signal Transduction Pathway that Modulates rhl Quorum Sensing and Bacterial Virulence in Pseudomonas aeruginosa. *PLoS pathogens* 10(8):e1004340.
13. Vilhelmsson O & Miller KJ (2002) Humectant permeability influences growth and compatible solute uptake by Staphylococcus aureus subjected to osmotic stress. *Journal of food protection* 65(6):1008-1015.
14. Thammavongsa V, Kern JW, Missiakas DM, & Schneewind O (2009) Staphylococcus aureus synthesizes adenosine to escape host immune responses. *The Journal of experimental medicine* 206(11):2417-2427.
15. Shin SH, Lim Y, Lee SE, Yang NW, & Rhee JH (2001) CAS agar diffusion assay for the measurement of siderophores in biological fluids. *Journal of microbiological methods* 44(1):89-95.
16. Morrissey JA, Cockayne A, Hill PJ, & Williams P (2000) Molecular cloning and analysis of a putative siderophore ABC transporter from Staphylococcus aureus. *Infection and immunity* 68(11):6281-6288.
17. Friedman DB*, et al.* (2006) Staphylococcus aureus redirects central metabolism to increase iron availability. *PLoS pathogens* 2(8):e87.
18. Irizarry RA*, et al.* (2003) Exploration, normalization, and summaries of high density oligonucleotide array probe level data. *Biostatistics* 4(2):249-264.
19. Tusher VG, Tibshirani R, & Chu G (2001) Significance analysis of microarrays applied to the ionizing radiation response. *Proceedings of the National Academy of Sciences of the United States of America* 98(9):5116-5121.
20. Li D*, et al.* (2005) Induction of fibronectin adhesins in quinolone-resistant Staphylococcus aureus by subinhibitory levels of ciprofloxacin or by sigma B transcription factor activity is mediated by two separate pathways. *Antimicrobial agents and chemotherapy* 49(3):916-924.
21. Renzoni A*, et al.* (2004) Modulation of fibronectin adhesins and other virulence factors in a teicoplanin-resistant derivative of methicillin-resistant Staphylococcus aureus. *Antimicrobial agents and chemotherapy* 48(8):2958-2965.
22. Vaudaux P*, et al.* (2002) Increased expression of clumping factor and fibronectin-binding proteins by hemB mutants of Staphylococcus aureus expressing small colony variant phenotypes. *Infection and immunity* 70(10):5428-5437.
23. Lan L*, et al.* (2004) Monitoring of gene expression profiles and isolation of candidate genes involved in pollination and fertilization in rice (Oryza sativa L.) with a 10K cDNA microarray. *Plant molecular biology* 54(4):471-487.
24. Livak KJ & Schmittgen TD (2001) Analysis of relative gene expression data using real-time quantitative PCR and the 2(-Delta Delta C(T)) Method. *Methods* 25(4):402-408.
25. Doublie S (1997) Preparation of selenomethionyl proteins for phase determination. *Methods in enzymology* 276:523-530.
26. Otwinowski Z & Minor W (1997) Processing of X-ray diffraction data collected in oscillation mode. *Method Enzymol* 276:307-326.
27. Collaborative Computational Project N (1994) The CCP4 suite: programs for protein crystallography. *Acta crystallographica. Section D, Biological crystallography* 50(Pt 5):760-763.
28. Sheldrick GM (2010) Experimental phasing with SHELXC/D/E: combining chain tracing with density modification. *Acta crystallographica. Section D, Biological crystallography* 66(Pt

4):479-485.
29. Emsley P & Cowtan K (2004) Coot: model-building tools for molecular graphics. *Acta crystallographica. Section D, Biological crystallography* 60(Pt 12 Pt 1):2126-2132.
30. Murshudov GN, Vagin AA, & Dodson EJ (1997) Refinement of macromolecular structures by the maximum-likelihood method. *Acta crystallographica. Section D, Biological crystallography* 53(Pt 3):240-255.
31. Duthie ES & Lorenz LL (1952) Staphylococcal coagulase; mode of action and antigenicity. *Journal of general microbiology* 6(1-2):95-107.
32. Fey PD*, et al.* (2013) A genetic resource for rapid and comprehensive phenotype screening of nonessential Staphylococcus aureus genes. *mBio* 4(1):e00537-00512.
33. Kreiswirth BN*, et al.* (1983) The toxic shock syndrome exotoxin structural gene is not detectably transmitted by a prophage. *Nature* 305(5936):709-712.
34. Notredame C, Higgins DG, & Heringa J (2000) T-Coffee: A novel method for fast and accurate multiple sequence alignment. *Journal of molecular biology* 302(1):205-217.
35. Gouet P, Robert X, & Courcelle E (2003) ESPript/ENDscript: Extracting and rendering sequence and 3D information from atomic structures of proteins. *Nucleic acids research* 31(13):3320-3323.
36. Hartmann T*, et al.* (2013) Catabolite control protein E (CcpE) is a LysR-type transcriptional regulator of tricarboxylic acid cycle activity in Staphylococcus aureus. *The Journal of biological chemistry* 288(50):36116-36128.